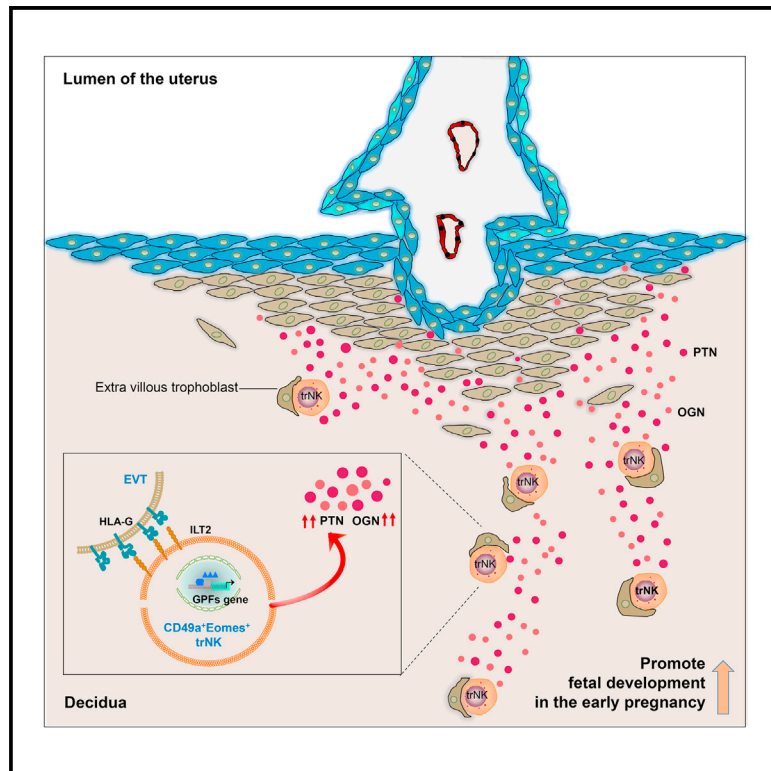


# Natural Killer Cells Promote Fetal Development through the Secretion of Growth-Promoting Factors

## Graphical Abstract



## Authors

Binqing Fu, Yonggang Zhou, Xiang Ni, ..., Rui Sun, Zhigang Tian, Haiming Wei

## Correspondence

tzg@ustc.edu.cn (Z.T.),  
ustcwhm@ustc.edu.cn (H.W.)

## In Brief

Maternal nourishment of the fetus at early stage has remained undefined. Fu et al. identify CD49a<sup>+</sup>Eomes<sup>+</sup> trNK cells in the uterus that secrete growth-promoting factors enhancing fetal growth during critical early stages of fetal development.

## Highlights

- Uterine CD49a<sup>+</sup>Eomes<sup>+</sup> trNK cell subset secretes GPFs including pleiotrophin and osteoglycin
- A decrease in the GPF-secreting trNK cell subset impairs fetal development
- Adoptive transfer of uterine-like trNK cells can reverse impaired fetal growth



# Natural Killer Cells Promote Fetal Development through the Secretion of Growth-Promoting Factors

Binqing Fu,<sup>1,2,5</sup> Yonggang Zhou,<sup>1,2,5</sup> Xiang Ni,<sup>1,2,5</sup> Xianhong Tong,<sup>3</sup> Xiuxiu Xu,<sup>1,2</sup> Zhongjun Dong,<sup>4</sup> Rui Sun,<sup>1,2</sup> Zhigang Tian,<sup>1,2,\*</sup> and Haiming Wei<sup>1,2,6,\*</sup>

<sup>1</sup>Institute of Immunology and the CAS Key Laboratory of Innate Immunity and Chronic Disease, School of Life Science and Medical Center, University of Science and Technology of China, Hefei, Anhui 230001, China

<sup>2</sup>Hefei National Laboratory for Physical Sciences at Microscale, University of Science and Technology of China, Hefei, Anhui 230001, China

<sup>3</sup>Anhui Provincial Hospital, Hefei, Anhui 230001, China

<sup>4</sup>School of Medicine, Tsinghua University, Beijing 100086, China

<sup>5</sup>These authors contributed equally

<sup>6</sup>Lead Contact

\*Correspondence: [tzg@ustc.edu.cn](mailto:tzg@ustc.edu.cn) (Z.T.), [ustcwhm@ustc.edu.cn](mailto:ustcwhm@ustc.edu.cn) (H.W.)

<https://doi.org/10.1016/j.immuni.2017.11.018>

## SUMMARY

Natural killer (NK) cells are present in large populations at the maternal-fetal interface during early pregnancy. However, the role of NK cells in fetal growth is unclear. Here, we have identified a CD49a<sup>+</sup>Eomes<sup>+</sup> subset of NK cells that secreted growth-promoting factors (GPFs), including pleiotrophin and osteoglycin, in both humans and mice. The crosstalk between HLA-G and ILT2 served as a stimulus for GPF-secreting function of this NK cell subset. Decreases in this GPF-secreting NK cell subset impaired fetal development, resulting in fetal growth restriction. The transcription factor Nfil3, but not T-bet, affected the function and the number of this decidual NK cell subset. Adoptive transfer of induced CD49a<sup>+</sup>Eomes<sup>+</sup> NK cells reversed impaired fetal growth and rebuilt an appropriate local microenvironment. These findings reveal properties of NK cells in promoting fetal growth. In addition, this research proposes approaches for therapeutic administration of NK cells in order to reverse restricted nourishments within the uterine microenvironment during early pregnancy.

## INTRODUCTION

Normal pregnancy is an intricately orchestrated process that requires both promotion of fetal growth and maintenance of immune tolerance. Among immune cells, uterine NK (uNK) cells are the most distinguishable lymphocytes during the first trimester of pregnancy, constituting >70% of all leukocytes in human deciduas (Jabrane-Ferrat and Siewiera, 2014). uNK cells exist only during early pregnancy and decrease after the placenta is formed. Interactions of NK cell-specific receptors with their ligands expressed on either invasive decidual stromal cells or trophoblasts orchestrate uterine NK cells with unique functional capabilities, including the promotion of placental vascular growth, decidualization, trophoblast invasion, and

immune balance (Colucci and Kieckbusch, 2015; Eberl et al., 2015; Nagashima et al., 2013; Rajagopalan, 2014; Zhang et al., 2011). The production of angiogenesis-regulating molecules, cytokines, and chemokines further exerts a positive impact on the placentation and birth weight (Hanna et al., 2006; Lash et al., 2006). Despite characterization and association between uNK cells and fetal growth restriction (FGR) in the interleukin-15-deficient (*IL-15*<sup>-/-</sup>) mouse (Barber and Pollard, 2003) and the transcription factor Nfil3-deficient (*Nfil3*<sup>-/-</sup>) mouse (Boulenouar et al., 2016) models, identification of the uNK cell subsets responsible for promoting fetal growth during early pregnancy are lacking. It has been reported that the presence and function of uNK cells may be correlated with fetal body weight. The interaction between activation receptor KIR2DS1 and HLA-C2 positively impacts birth weight, whereas the interaction of the inhibitory receptor KIR2DL1 with HLA-C2 negatively impacts birth weight (Hiby et al., 2010, 2014).

uNK cells have been studied for decades as an example of specialized immune cells endowed with angiogenic and regulatory activities that develop during the evolution of mammalian pregnancy. However, whether these transient NK cells participate in the early optimization of maternal nourishment of the fetus remains unknown. In a previous report, we identified that uNK cells function as key regulatory cells but do not destroy cells at the maternal-fetal interface (Fu et al., 2013, 2014a, 2014b). Here, we examined whether CD49a<sup>+</sup> uNK cells are responsible for maintaining the nourishing function in the early fetus.

## RESULTS

### Uterine trNK Cells Secrete Growth-Promoting Factors (GPFs)

Uterine NK cells have a series of characteristics similar to traditional NK cells, including the expression of CD56 and NK receptors, such as NKp30, NKp46, NKp44, and NKG2D. Likewise, uNK cells also express unusual lectin-like receptors such as NKG2E, multiple tetraspanins (CD9, CD53, CD151, CD63, and TSPAN-5), several killer cell Ig-like receptors (KIR), and integrin subunits (Zhang et al., 2017; Koopman et al., 2003). Previously, it was shown that there are CD49a<sup>+</sup> tissue-resident NK cell



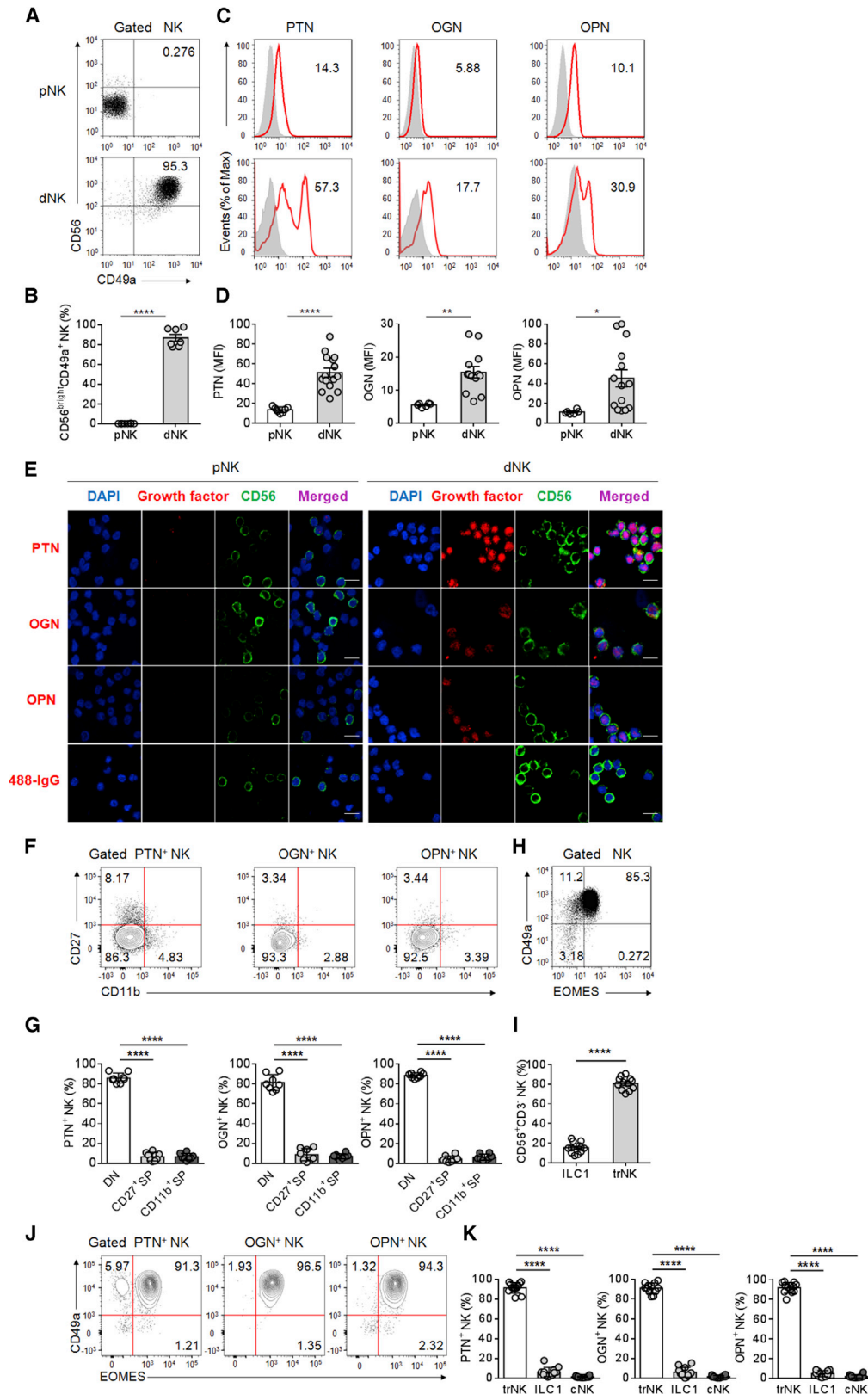


**Figure 1. Identification of GFP Secretion in Human CD49a<sup>+</sup>Eomes<sup>+</sup> trNK Cells**

(A) Representative density plots showing an analysis of CD56 and CD49a expressions in gated CD45<sup>+</sup>CD56<sup>+</sup>CD3<sup>-</sup> NK cells isolated from peripheral blood and decidua in the first trimester. Data are representative of three independent experiments.

(legend continued on next page)

subsets in mouse liver but there is an even larger population in the uterus (Peng et al., 2013; Sojka et al., 2014). Comparing human uterine CD49a<sup>+</sup> NK cell subsets to NK cell subsets stratified by CD16, CD27, and CD11b (Fu et al., 2011, 2014a), human CD49a expression in NK cells were analyzed from decidua of the first trimester compared to those from peripheral blood. In human decidual NK (dNK) cells, more than 85% of NK cells (gated CD45<sup>+</sup>CD56<sup>+</sup>CD3<sup>-</sup>) expressed CD49a (Figures 1A and 1B), where most of the CD49a<sup>+</sup> NK cells were CD16<sup>-</sup>CD56<sup>bright</sup> NK cells and both the CD27<sup>-</sup>CD11b<sup>-</sup> and CD27<sup>+</sup>CD11b<sup>-</sup> subsets were included (Figures S1A and S1B).

To identify genes promoting fetal development in early pregnancy, gene expression was measured in sorted CD49a<sup>+</sup> NK cells from deciduas in the first trimester of pregnancy compared with the sorted CD49a<sup>-</sup> NK cells from peripheral blood. We observed the upregulation of a set of genes that were previously identified as key regulators during pregnancy, such as *VEGF*, *IGF2*, and *ITGAD* (Kalkunte et al., 2009; Mansell et al., 2016; Vacca et al., 2013). We further identified that CD49a<sup>+</sup> NK cells upregulated several GPFs, including pleiotrophin (PTN, encoded by *PTN*), osteoglycin (OGN, encoded by *OGN*) and osteopontin (OPN, encoded by *SPP1*), compared to these products in CD49a<sup>-</sup> NK cells (Figures S1C–S1F). These GPFs are critical for the development of blood vessels, bone, cartilage, neurite, and cardiac tissue in the fetus (Choi et al., 2008; Sarwar et al., 2009; Singh et al., 2014). In Figure S1G, the expression of GPFs was determined by analyzing RNA expression in purified CD49<sup>+</sup> NK cells and CD49a<sup>-</sup> NK cells. Further protein analyses using both flow cytometry and immunofluorescence demonstrated that dNK cells had higher expressions of PTN, OGN, and OPN than pNK cells (Figures 1C–1E). To determine which subset was the main source of GPFs, we gated each subset of GPF<sup>+</sup> NK cells and further showed the expression of CD27 and CD11b (Figures 1F and 1G). All the PTN<sup>+</sup> NK, OGN<sup>+</sup> NK, and OPN<sup>+</sup> NK cells primarily existed within the CD27<sup>-</sup>CD11b<sup>-</sup> NK cell subset. It has been reported that CD49a<sup>+</sup> NK cells from mouse uterus have two distinct subsets: CD49a<sup>+</sup>Eomes<sup>-</sup> innate lymphoid cells 1 (ILC1s) and CD49a<sup>+</sup>Eomes<sup>+</sup> uterus tissue-resident NK (trNK) cells (Doisne et al., 2015). To investigate trNK cell subsets in human deciduas and to identify the main source of GPFs, it was first verified that in human deciduas, >80% of the dNK cells co-expressed CD49a and Eomes, belonging to the

trNK cell subset, and that <20% of the dNK cells were ILC1s (Figures 1H and 1I). Next, each kind of GPF<sup>+</sup> NK cell was gated showing that the CD49a<sup>+</sup>Eomes<sup>+</sup> trNK cells were the main source of GPFs, including PTN, OGN, and OPN, as compared to ILC1s and conventional CD49a<sup>-</sup>Eomes<sup>+</sup> NK (cNK) cell subsets (Figures 1J and 1K). Taken together, these results indicate that decidual NK cells, especially those in the CD49a<sup>+</sup>Eomes<sup>+</sup> trNK cell subsets, secrete GPFs.

### HLA-G Induces NK Cells to Secrete GPFs

Feto-maternal crosstalk is critical for the activation of immune cells as well as in maintaining the health of the offspring (Arck and Hecher, 2013). To determine whether stimulation from the fetus affects GPFs secreted by dNK cells, we purified human dNK cells, co-cultured them with extravillous trophoblast (EVT) cells, and compared them in the presence and absence of the mitogen, PMA. The data revealed that dNK cells secreted more GPFs, including PTN, OGN, and OPN, upon co-stimulation with EVT cells compared with the other two groups (Figures 2A and 2B). Additionally, high expressions of HLA molecules on fetal trophoblast cells and their receptors on maternal uterine NK cells are critical for initiating and promoting immune functions (Kieckbusch et al., 2014; Male et al., 2011; Tilburgs et al., 2015; Xiong et al., 2013). Among these HLAs, HLA-G is the only HLA that is specifically expressed in fetal-derived trophoblast cells. Thus, we further investigated whether crosstalk existed between HLA-G and KIR receptors in promoting GPF secretion. First, a co-culture system was constructed including purified human dNK cells and 721.221 (an MHC class I-negative human B cell line) transfected with cDNAs encoding either HLA-G or HLA-C (Figures S2A–S2C). Both HLA-G and HLA-C expression were analyzed in 721.221-HLA-G and 721.221-HLA-C to ensure that HLA-C has a similarly high expression as HLA-G in transfected cells (Figures S2D and S2E). As a result, the transduced dNK cells possessed a stronger ability to secrete GPFs after co-culturing with 721.221-HLA-G compared to corresponding dNK cells co-cultured with either 721.221-HLA-C or control cultures (Figure 2C). These data indicate that HLA-G, but not HLA-C, promotes GPF secretion in dNK cells.

HLA-G has been reported to bind to the immunoglobulin-like transcript receptors 2 and 4 (ILT2 and ILT4) (LeMaout et al., 2005), CD8 (Sanders et al., 1991), and the activation receptor

(B) Percentages of CD56<sup>bright</sup>CD49a<sup>+</sup> NK cell subsets in gated CD56<sup>+</sup>CD3<sup>-</sup> pNK and dNK cells. n = 8 and 7 for pNK and dNK cells, respectively. Unpaired t test.

(C) Flow cytometry of GPFs expressions in pNK cells and dNK cells.

(D) Statistics calculated by the MFI of each GPF from pNK and dNK cells. n = 6–8 and 13–15 for pNK and dNK cells, respectively. Unpaired t test.

(E) Confocal microscopy of the expressions of GPFs in sorted pNK cells and dNK cells. Scale bar, 10 μm. Data are representative of two independent experiments.

(F–K) NK cells are isolated from normal deciduas in the first trimester and first gated as CD45<sup>+</sup>CD56<sup>+</sup>CD3<sup>-</sup> NK cells.

(F) Representative density plots showing an analysis of CD27 and CD11b expressions in further gated GPF<sup>+</sup> NK cells (gated PTN<sup>+</sup> NK cells, OGN<sup>+</sup> NK cells, and OPN<sup>+</sup> NK cells separately). Data are representative of two independent experiments.

(G) Percentages of GPF<sup>+</sup> NK cells in uterus DN (CD27<sup>-</sup>CD11b<sup>-</sup> NK) cell subsets, CD27<sup>+</sup> SP (CD27<sup>+</sup>CD11b<sup>-</sup> NK) cell subset, and CD11b<sup>+</sup> SP (CD27<sup>-</sup>CD11b<sup>+</sup> NK) cell subset. n = 8. Paired t test.

(H) Representative density plots showing an analysis of CD49a and Eomes expressions in gated CD45<sup>+</sup>CD56<sup>+</sup>CD3<sup>-</sup> dNK cells. Data are representative of two independent experiments.

(I) Percentages of uterus trNK cell subsets (CD49a<sup>+</sup>Eomes<sup>+</sup>) and ILC1 subsets (CD49a<sup>+</sup>Eomes<sup>-</sup>) in gated dNK cells. n = 12. Paired t test.

(J) Representative density plots showing an analysis of CD49a and Eomes expressions in further gated GPF<sup>+</sup> NK cells. Data are representative of two independent experiments.

(K) Percentages of GPF<sup>+</sup> NK cells in uterus trNK cell subsets, ILC1 subset, and cNK (CD49a<sup>-</sup>Eomes<sup>+</sup>) cell subset. n = 12. Paired t test.

The numbers in (A), (F), (H), and (J) show the percentage of each indicated NK cell subset. The numbers in (C) show the mean MFI of each GPF expression. Mean ± SEM, \*p < 0.05, \*\*p < 0.01, \*\*\*p < 0.005, \*\*\*\*p < 0.0001. See also Figure S1.

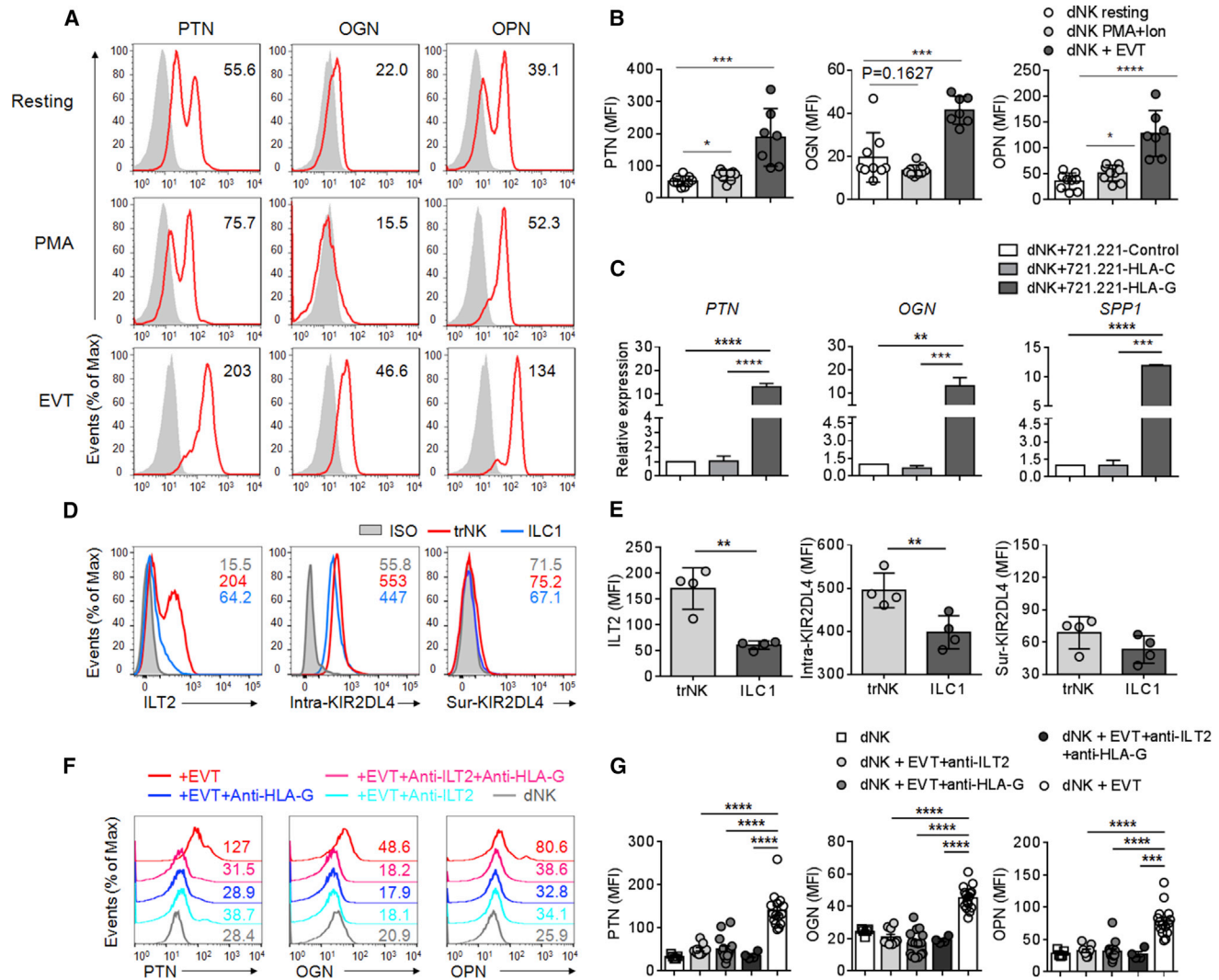


**Figure 2. HLA-G-ILT2 Crosstalk Induces Uterine NK Cell Upregulation of GPFs**

(A) Flow cytometry of GPFs expressions in purified dNK cells co-culture with EVT cells or PMA or no stimulation. EVT cells were co-cultured with dNK cells at a ratio of 1:20.

(B) Statistics calculated by the MFI of each GPF from dNK cells co-cultured with EVT cells or PMA or no stimulation.  $n = 7-9$ . Unpaired t test.

(C) Quantitative RT-PCR of GPF genes in dNK cells co-cultured with 721.221 cells or 721.221-HLA-C or 721.221-HLA-G cells, normalized to their expressions in dNK cells alone. Unpaired t test.

(D) Flow cytometry of ILT2, intracellular KIR2DL4, and surface KIR2DL4 on gated  $CD45^+CD56^+CD3^-$  dNK cells from the first trimester.

(E) Statistics calculated by the MFI of each ILT2, intracellular KIR2DL4, and surface KIR2DL4 on gated trNK ( $CD49a^+Eomes^-$ ) cell subset and ILC1 ( $CD49a^+Eomes^-$ ) cell subset.  $n = 4$ . Paired t test.

(F) Flow cytometry of GPFs expressions in purified dNK cells from the first trimester co-cultured with EVT cells with or without anti-HLA-G or anti-ILT2.

(G) Statistics calculated by the MFI of each GPF from dNK cells co-cultured with EVT cells with or without anti-HLA-G or anti-ILT2.  $n = 5-15$ . Unpaired t test.

The numbers in (A), (D), and (F) show the mean MFI of each indicated protein expression. Mean  $\pm$  SEM. See also Figure S2.

KIR2DL4 (Rajagopalan and Long, 2012). To determine which receptor is involved in the crosstalk with HLA-G, the expression of these receptors was analyzed in dNK cells. No expression of ILT4 or CD8 was found on dNK cells (Figures S2F and S2G). Expression of surface ILT2 and intracellular KIR2DL4 were observed in dNK cells. Specifically, the trNK cell subset had higher expressions of ILT2 and intracellular KIR2DL4 than the ILC1 subset (Figures 2D and 2E). To identify whether the crosstalk between HLA-G and ILT2 play a role in triggering the GPF-secreting function of NK cells, another co-culture system was constructed comprising

purified human dNK cells and EVT cells in the presence or absence of anti-HLA-G antibody and anti-ILT2 antibodies. Significantly lower expression of PTN, OGN, and OPN was measured in groups treated with the anti-HLA-G antibody, the anti-ILT2 antibody, or both antibodies, indicating that HLA-G-ILT2 crosstalk activates GPF secretion (Figures 2F and 2G). Moreover, the only known ligand for KIR2DL4 is HLA-G. To determine whether KIR2DL4 promotes GPF secretion, purified dNK cells were transfected with siRNA either targeting KIR2DL4 or present as a null vector, and then co-cultured with fetal EVT cells. GPFs

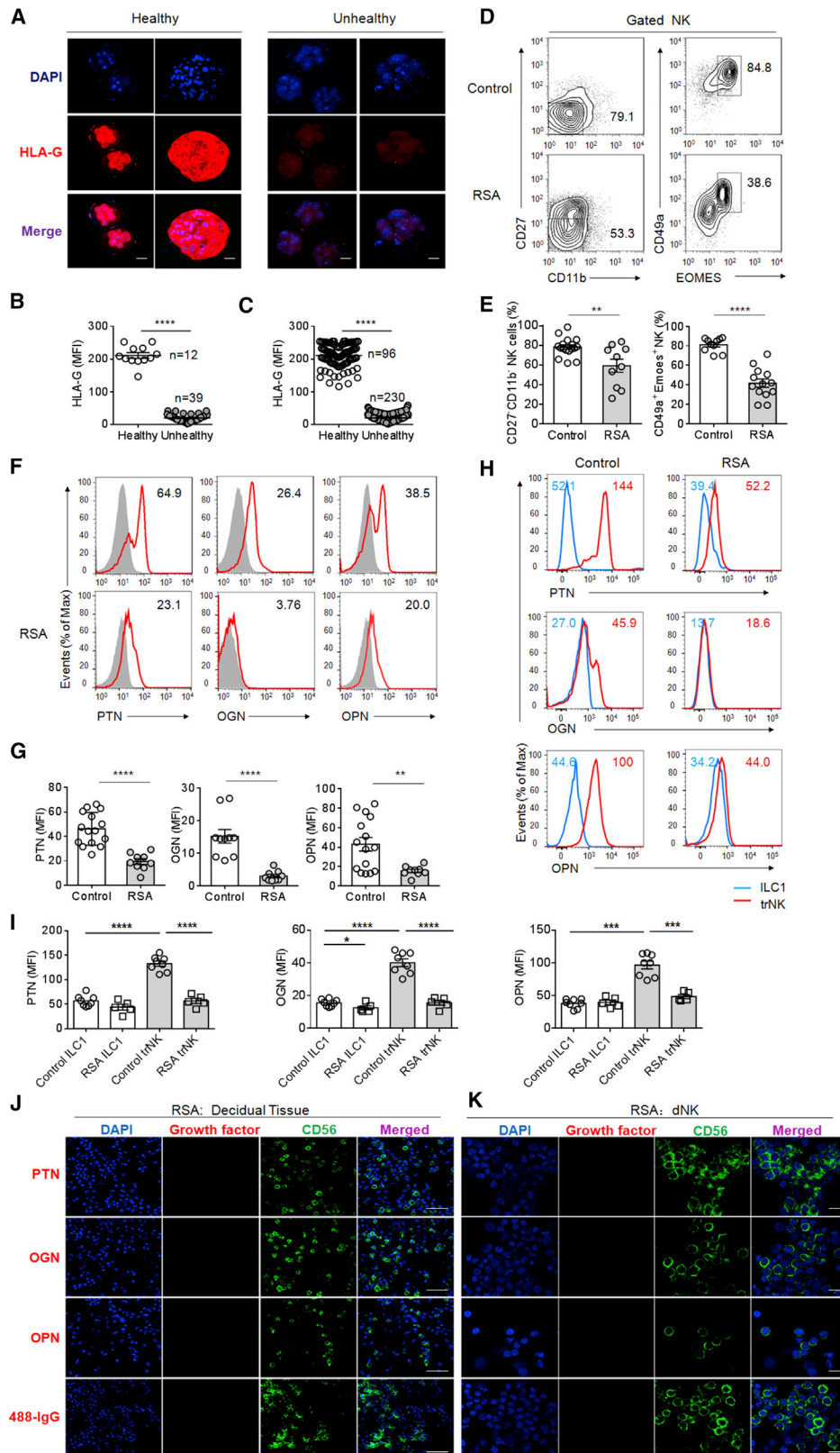


**Figure 3. Decreased trNK Cells and Impaired GPFs in RSA Patients**

(A) Confocal microscopy of the expressions of HLA-G in normal or abnormal morulas which have non-integer cleavage obtained from *in vitro* fertilization. The scale bar = 50  $\mu$ m.

(legend continued on next page)

significantly decreased in cells transfected with siRNA of KIR2DL4 groups compared to controls (Figures S2H and S2I). These data show that the HLA-G-ILT2-KIR2DL4 axis is essential in GPF secretion from dNK cells in early pregnancy.

### Impaired GPF<sup>+</sup> NK Cells in Patients with Fetal Loss

HLA-G promotes trNK cell-driven GPF secretion in embryonic development. Thus, HLA-G expression was investigated between normal morulas and abnormal morulas that display non-integer cleavage obtained from *in vitro* fertilization. Similar to previous reports (Jurisicova et al., 1996; Sun et al., 2011), normal morulas were found to have significantly higher expressions of HLA-G than abnormal morulas (Figures 3A–3C), indicating that HLA-G expression prepares for normal pre-implantation. To determine whether GPF-secreting NK cells changed phenotype and function in patients, dNK cells were analyzed from patients experiencing recurrent spontaneous abortion (RSA) with a normal embryonic karyotype. Decidual NK cells from healthy females showed a large population of CD27<sup>+</sup>CD11b<sup>+</sup> (78.12% ± 2.294%) and CD49a<sup>+</sup>Eomes<sup>+</sup> (81.17% ± 2.216%) trNK cell subsets. However, dNK cells from RSA patients exhibited a significantly decreased percentage of CD27<sup>+</sup>CD11b<sup>+</sup> (59.16% ± 6.650%) and CD49a<sup>+</sup>Eomes<sup>+</sup> (41.75% ± 4.299%) trNK cell subsets (Figures 3D and 3E). Furthermore, contrary to the high GPF expression in normal dNK cells, significantly decreased expression of GPFs, including PTN, OGN, and OPN, were confirmed in dNK cells from RSA patients via flow cytometry (Figures 3F and 3G). The loss of growth factor production was either due to a change in the distribution of cell populations in the uterus or due to an inability to produce growth factor. Thus, growth factor production was compared in both ILC1 and trNK cell subsets from decidua samples in the first trimester from healthy donors and RSA patients. trNK cell subsets from deciduas of RSA patients showed less capability to produce growth factors compared to those from the healthy controls (Figures 3H and 3I). Immunofluorescence of both decidual tissues and purified dNK cells from RSA patients showed little GPF expression (Figures 3J and 3K). Thus the change in the distribution of cell populations in the uterus and the inability to produce growth factor contribute to less growth factor production in RSA patients. Therefore, insufficient secretion of GPFs from dNK cells, as well as insufficient crosstalk between maternal NK cells and fetal cells, may be responsible for the confined fetal development.

### Lack of GPF<sup>+</sup> trNK Cells Results in Fetal Growth Restriction

Our results showed that insufficient secretion of GPFs from dNK cells have connected with confined fetal development in human. These results raised the question whether mouse trNK cells also have ability to secrete GPFs and whether a lack of trNK cells could affect fetal development. In order to address this question, NK cell genetically deleted mice including *Nfil3*<sup>-/-</sup> and *Tbx21*<sup>-/-</sup> mice were used. Since in humans many birth defects and pregnancy complications are more frequent in older mothers, aged mice models were also included to investigate trNK cell subsets from the uteruses. As a result, the number of CD49a<sup>+</sup>Eomes<sup>+</sup> trNK cells isolated from the uterus of *Nfil3*<sup>-/-</sup> mice was significantly downregulated during pregnancy (Figures 4A, 4B, and S3A). To determine whether trNK cells are the main source of GPFs in mice, PTN-, OGN-, and OPN-positive NK cells were gated showing that, similar to trNK cells in humans, trNK cells in mice exhibited the strongest capability to secrete GPFs compared to ILC1 and cNK cell subsets (Figures S3B and S3C). Analysis of GPF<sup>+</sup>Eomes<sup>+</sup> NK cells within the CD49a<sup>+</sup> gated dNK cell population on gd10.5 showed that all three GPFs significantly decreased in *Nfil3*<sup>-/-</sup> mice compared to B6 controls (Figures 4C and 4D). The RNA expression of *Ptn*, *Ogn*, and *Spp1* also significantly decreased in uteruses of *Nfil3*<sup>-/-</sup> mice compared to B6 controls (Figure 4E).

To further determine whether the reduced function of GPF-secreting trNK cells affects fetal growth and to verify the impact of maternal or paternal elements on fetal growth, we created three experimental groups: group A (B6 female mated with a B6 male), group B (B6 female mated with an *Nfil3*<sup>-/-</sup> male), and group C (*Nfil3*<sup>-/-</sup> female mated with a B6 male). In these three groups, fetal observations revealed that among age-matched fetuses, the weights were significantly decreased in group C, indicating severe FGR in fetuses from pregnant *Nfil3*<sup>-/-</sup> mice (Figures 4F–4I). The fetal weights from group D (*Nfil3*<sup>-/-</sup> female mated with an *Nfil3*<sup>-/-</sup> male) were similarly decreased as observed in group C (Figures S3D and S3E). The development of the fetal skeletal system is an important index for evaluating fetal growth. Skeletons were prepared from embryos and stained with Alizarin red and Alcian blue dyes, which detect bone and cartilage tissue, respectively. As shown in Figure 4J, skeletons from groups A and B showed gradual ossification in the skull, clavicles, vertebral arches, scapulae, ribs, pelvis, long bones, metatarsals, and metacarpals during pregnancy. In contrast,

(B) Statistics calculated by the mean MFI of HLA-G from normal or abnormal morulas. n = 12 and 39, respectively. Unpaired t test.

(C) Statistics calculated by the MFI of HLA-G from randomly selected single blastomeres from each normal or abnormal morula. n = 96 and 230, respectively. Unpaired t test.

(D) Representative density plots showing an analysis of CD27 and CD11b expressions (left) and CD49a and Eomes expressions (right) in gated CD45<sup>+</sup>CD56<sup>+</sup>CD3<sup>-</sup> dNK cells isolated from normal decidua or deciduas from RSA patients.

(E) Statistics calculated by the percentages of CD27<sup>+</sup>CD11b<sup>+</sup> NK cells (left) and CD49a<sup>+</sup>Eomes<sup>+</sup> trNK cells (right) from normal dNK cells and RSA dNK cells. n = 10–17, unpaired t test.

(F) Flow cytometry of GPFs expressions in CD56<sup>+</sup>CD3<sup>-</sup> dNK cells from normal or RSA deciduas.

(G) Statistics calculated by the MFI of each GPF from dNK cells from normal or RSA deciduas. n = 10–14 and 9, respectively. Unpaired t test.

(H) Flow cytometry of GPFs expressions in gated ILC1s and trNK cells from normal dNK cells and RSA dNK cells.

(I) Statistics calculated by the MFI of each GPF from ILC1s and trNK cells from normal or RSA deciduas. n = 5–8, unpaired t test.

(J and K) Confocal microscopy of the expressions of GPFs in decidual tissues (J) and sorted dNK cells (K) from RSA patients. Scale bar in (J) = 50 μm, in (K) = 10 μm.

The numbers in (D) show the percentage of each indicated NK subsets. The numbers in (F) and (H) show the mean MFI of each GPF expression. Mean ± SEM, \*p < 0.05, \*\*p < 0.01, \*\*\*p < 0.005, \*\*\*\*p < 0.0001. See also Table S1.

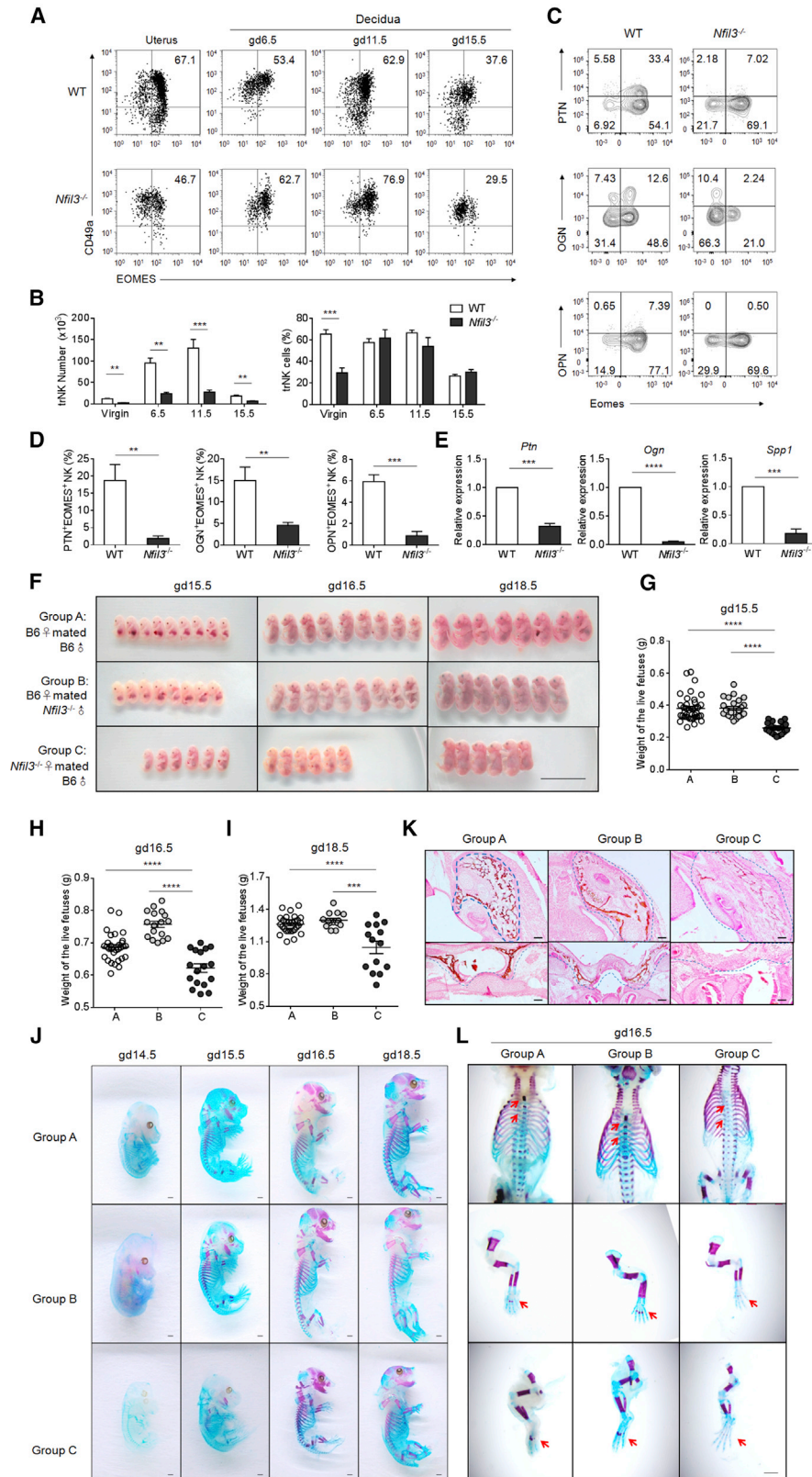


**Figure 4. Decreased trNK Cells, Impaired GPFs, and FGR in Pregnant *Nfil3*<sup>-/-</sup> Mice**

(A) Flow cytometry of CD49a and Eomes expressions in NK1.1<sup>+</sup>CD3<sup>-</sup>CD19<sup>-</sup> NK cells in virgin uterus, deciduas at gestation day 6.5, 11.5, 15.5 from WT mice and *Nfil3*<sup>-/-</sup> mice.

(legend continued on next page)

skeletons from group C at the same embryonic age exhibited a much smaller size and reduced mineralized bone tissue that should stain red. Specifically, skeletons from group C at gd15.5 exhibited less mineralized bone tissue in skull, vertebral arches, ribs, clavicles, tibia, and radius (Figure S3F). Histological examination of the skull at gd16.5 revealed that bone formation was poor in fetuses from group C compared to those in the other two groups (Figure 4K). Skeletons from group C at gd16.5 exhibited an almost complete lack of mineralized bone tissue in the sternum and lower amounts of mineralized bone tissue in the metacarpals and metatarsals compared to groups A and B (Figure 4L). Notably, only *Nfil3* deficiency from the maternal contribution but not the paternal contribution affected the pregnancy outcomes.

T-bet is a key transcriptional factor of CD49a<sup>+</sup> NK cells in the liver (Sojka et al., 2014). To assess whether T-bet affects uterus trNK cell and fetal growth, the CD49a<sup>+</sup> NK cell subset was evaluated in uteruses from *Tbx21*<sup>-/-</sup> mice. Consistent with a previous report (Sojka et al., 2014), *Tbx21*<sup>-/-</sup> mice had a high percentage of uterine CD49a<sup>+</sup> NK cells, similar to normal B6 mice (Figure S4A). Contrary to *Nfil3*<sup>-/-</sup> mice, *Tbx21*<sup>-/-</sup> mice had a similar number of CD49a<sup>+</sup>Eomes<sup>+</sup> trNK cells (Figure S4B). Analysis of GPFs in the uteruses from *Tbx21*<sup>-/-</sup> mice exhibited no differences compared with normal B6 mice (Figure S4C). Specifically, no significant changes were found in the number of live fetuses and the fetal weight between *Tbx21*<sup>-/-</sup> mice and B6 controls (Figures S4D–S4F). In addition, no change was observed in the mineralized bone tissues in fetuses from *Tbx21*<sup>-/-</sup> mice and from B6 controls (Figures S4G and S4H). Overall, these data reveal that *Nfil3* but not T-bet are critical for the existence of GPF<sup>+</sup> trNK cell subsets.

Advanced maternal age is an independent risk factor for abnormal pregnancy (Jolly et al., 2000; Schulkey et al., 2015). However, whether an aged pregnancy affects CD49a<sup>+</sup>Eomes<sup>+</sup> trNK cells as well as fetal growth has not been elucidated. Uteruses from female primiparous B6 mice between 11 and 14 months in age were analyzed. Notably, the number of CD49a<sup>+</sup> NK cells in the uteruses from aged mice was decreased compared to that in normal controls (Figure S5). No differences in the number of CD49a<sup>+</sup>Eomes<sup>+</sup> trNK cells were found in the deciduas of aged mice compared to controls during pregnancy (Figures 5A and 5B). However, further analysis of these GPF<sup>+</sup>Eomes<sup>+</sup> NK cells in CD49a<sup>+</sup> gated dNK cells at gd10.5 showed that GPFs significantly decreased in uteruses from aged mice compared to B6 controls during pregnancy (Figures 5C and 5D). RNA expression of *Ptn* and *Ogn* significantly decreased in the uteruses of aged mice compared to B6 controls (Figure 5E). Thus the function of GPF

secretion from NK cells is impaired in aged mice. Additionally, both the weight of the uterus and live fetuses decreased in aged pregnancies compared to the normal controls (Figures 5F–5H). The skeletons of the embryos from aged females were much smaller in size with profound absence of mineralized bone tissue that should stain red in the sternum and much lower amounts of mineralized bone tissue in the metacarpals and metatarsals (Figure 5I). Histological examinations of the skull at gd16.5 showed that bone formation was poor in fetuses from aged females compared to normal controls (Figure 5J). Therefore, reduced trNK cell subsets and impaired GPFs secretion from *Nfil3*<sup>-/-</sup> mice and aged mice are accompanied by a remarkable FGR and defective development of the fetal skeletal system.

### Transfer-Induced trNK Cells Rescues Fetal Growth

A decrease in trNK cells in the uterus may cause severe FGR in *Nfil3*<sup>-/-</sup> mice (Figure 4) and in aged mice (Figure 5). Thus, it was investigated whether transferring induced uterus-like trNK cells to supply enough GPFs for fetal growth would reverse the pregnancy outcome. First, an *in vitro* culture and amplification system of CD49a<sup>+</sup> NK cells was administered. After 30 days of culture, a large number of NK cells were induced, and more than 90% of these NK1.1<sup>+</sup>CD3<sup>-</sup> NK cells expressed the CD49a marker (Figure 6A). Induced CD49a<sup>+</sup> NK cells presented high expressions of CD69, NKG2A, and Eomes, similar to the phenotype of uterine trNK cells (Figure 6B). Further analysis revealed that induced NK cells had a high GPF expression (Figure 6C). Transferring induced CD49a<sup>+</sup> NK cells from CD45.2 B6 mice into CD45.1 recipient mice showed that induced CD49a<sup>+</sup> NK cells could reach the uterus (Figures 6D and 6E). To determine whether induced CD49a<sup>+</sup> uterus-like NK cells could reverse the poor pregnancy results in *Nfil3*<sup>-/-</sup> mice, adoptive transfer experiments were performed by transferring the induced CD49a<sup>+</sup> uterus-like NK cells (1 × 10<sup>6</sup> cells/mouse) into a pregnant *Nfil3*<sup>-/-</sup> mouse at gd6.5. In the group of pregnant *Nfil3*<sup>-/-</sup> mice that received the induced uterus-like CD49a<sup>+</sup> NK cells, FGR was alleviated compared to the non-transferred *Nfil3*<sup>-/-</sup> group and the *Nfil3*<sup>-/-</sup> group transferred with NK cells from the spleen (Figures 6F and 6G). Similarly, the weight of the fetuses from aged mice that were transferred with induced uterus-like CD49a<sup>+</sup> NK cells increased and FGR in the transferred group was alleviated compared to the non-transferred controls and those transferred with spleen NK cell groups (Figures 6H and 6I). Thus, transfer-induced uterus-like NK cells could constitute a practical and promising approach to reverse FGR accumulation in an abnormal uterus.

To further investigate whether this reversion of FGR by induced NK cells acts via GPFs, *Ptn*<sup>-/-</sup>*Ogn*<sup>-/-</sup>*Spp1*<sup>-/-</sup> mice

(B) Statistics calculated by the percentages and cell number of trNK (CD49a<sup>+</sup>Eomes<sup>+</sup>) cells from uterus of WT mice and *Nfil3*<sup>-/-</sup> mice. Unpaired t test.

(C) Flow cytometry of GPFs and Eomes expressions in CD49a<sup>+</sup>NK1.1<sup>+</sup>CD3<sup>-</sup>CD19<sup>-</sup> dNK cells from WT mice and *Nfil3*<sup>-/-</sup> mice at gd10.5.

(D) Statistics calculated by the percentage of each GPF<sup>+</sup>Eomes<sup>+</sup> subset from CD49a<sup>+</sup> dNK cells from WT mice and *Nfil3*<sup>-/-</sup> mice. n = 5–9, unpaired t test.

(E) Quantitative RT-PCR of GPFs genes in virgin uterus from WT mice and *Nfil3*<sup>-/-</sup> mice. Data are representative of two independent experiments. Unpaired t test.

(F) Representative picture of fetuses from groups A, B, and C at gd15.5, gd16.5, and gd18.5. Scale bar, 3 cm.

(G–I) Statistics calculated by the weight of fetuses in group A, B, and C at gd15.5 (n = 38, 25, 19, respectively), gd16.5 (n = 30, 17, 17 respectively), and gd18.5 (n = 28, 14, 14, respectively). \*\*\*p < 0.005, \*\*\*\*p < 0.0001, unpaired t test.

(J) Representative pictures of fetal skeletal staining of embryos from group A (B6 female mated B6 male), group B (B6 female mated *Nfil3*<sup>-/-</sup> male), and group C (*Nfil3*<sup>-/-</sup> female mated B6 male) at gd14.5, gd15.5, gd16.5, and gd18.5. Bars: 1 mm. Data are representative of three independent experiments.

(K) Von Kossa staining of skulls from groups A, B, and C at gd16.5. Bars: 100 μm.

(L) Stereomicroscope pictures of fetal skeletal staining of embryos from groups A, B, and C at gd16.5. Bars: 1 mm.

The numbers in (A) and (C) show the percentage of each indicated NK subsets. Mean ± SEM. See also Figures S3 and S4.

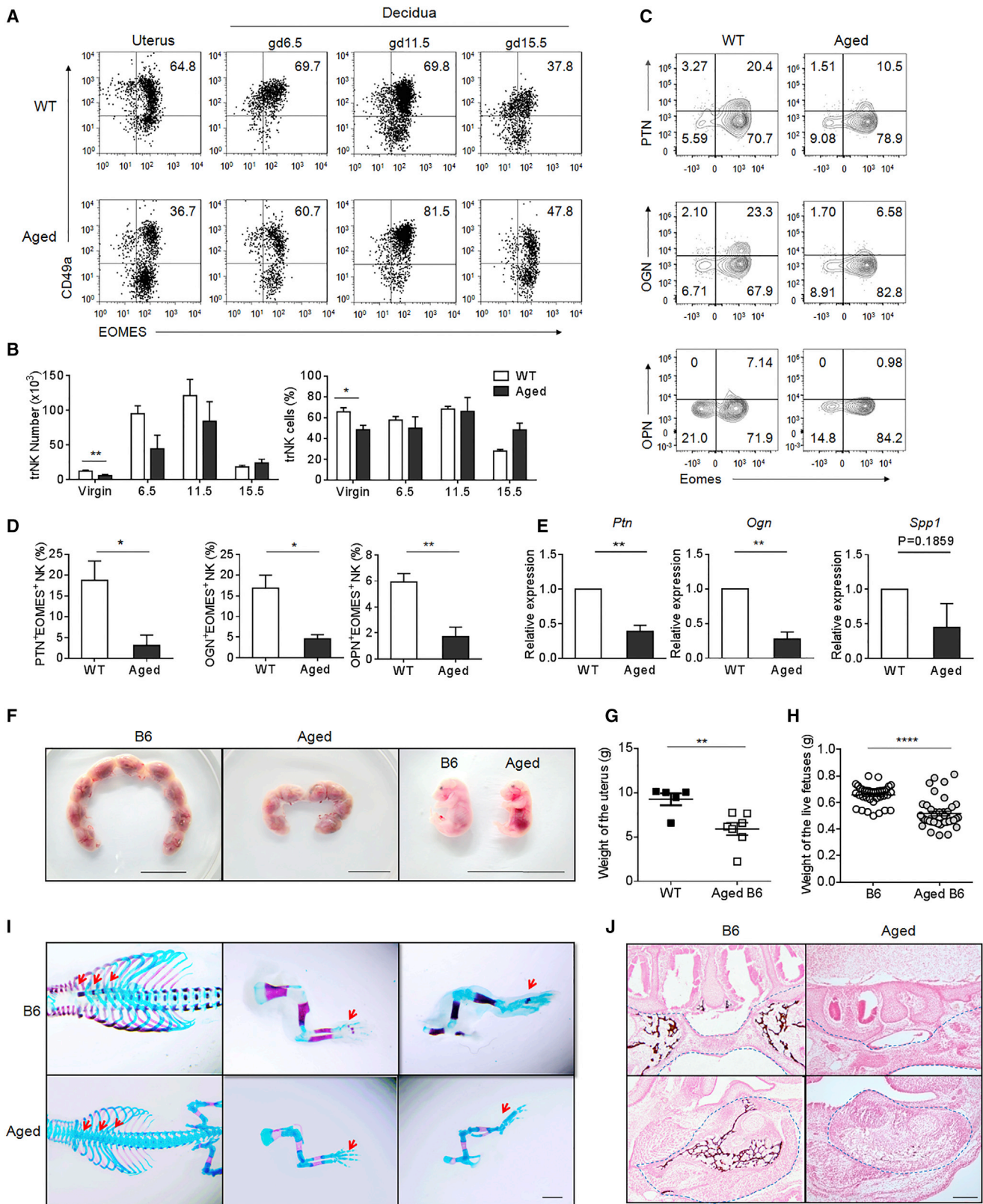


**Figure 5. Decreased trNK Cells, Impaired GPFs, and FGR in Pregnant Aged Mice**

(A) Representative density plots showing an analysis of CD49a and Eomes expressions in gated NK1.1<sup>+</sup>CD3<sup>-</sup>CD19<sup>-</sup> NK cells isolated from virgin uterus, deciduas at gestation day 6.5, 11.5, 15.5 of aged mice and control mice. Data are representative of two independent experiments.

(legend continued on next page)

were generated using CRISPR-Cas9 technology as described (Figures S6A and S6B; Niu et al., 2014; Wang et al., 2013). These *Ptn*<sup>-/-</sup>*Ogn*<sup>-/-</sup>*Spp1*<sup>-/-</sup> mice showed significantly decreased uterine weight and fewer live fetuses (Figures S6C–S6F), as well as impaired GPF expression (Figures S6G–S6I). Mouse bone marrow cells from *Ptn*<sup>-/-</sup>*Ogn*<sup>-/-</sup>*Spp1*<sup>-/-</sup> mice were amplified, sorted, and further differentiated into CD49a<sup>+</sup> uterus-like NK cells. To identify whether the induced NK cells from *Ptn*<sup>-/-</sup>*Ogn*<sup>-/-</sup>*Spp1*<sup>-/-</sup> mice have reduced migration ability towards the uterus, mouse bone marrow cells from *Ptn*<sup>-/-</sup>*Ogn*<sup>-/-</sup>*Spp1*<sup>-/-</sup> mice were amplified, sorted, differentiated into CD49a<sup>+</sup> uterus-like NK cells, and further adoptive transferred into CD45.1 recipient mice. These transferred NK cells could reach the uterus and had no significant differences compared to WT induced CD49a<sup>+</sup> NK cells in distribution (Figures 6D and 6E). Compared with the improved situation in the group that received a transfer of CD49a<sup>+</sup> uterus-like NK cells, the group that received a transfer of CD49a<sup>+</sup> uterus-like NK cells induced from *Ptn*<sup>-/-</sup>*Ogn*<sup>-/-</sup>*Spp1*<sup>-/-</sup> mice showed significantly decreased body weight, indicative of severe FGR disease (Figures 6J and 6K). To further investigate which specific GPFs are more dominant over others, blocking GPF antibodies were used. Development of fetuses was compared between the antibody groups and the IgG controls. The data showed a significantly decreased fetal weight from the anti-PTN and anti-OGN groups compared to the IgG controls (Figures 6L and 6M). This suggests that PTN and OGN are more important for NK cell-mediated fetal sustenance. Additionally, to verify whether injection of each of these growth factors can rescue fetal development, PTN, OGN, or OPN were intravenously injected in *Nfil3*<sup>-/-</sup> pregnant mice. Compared to the others, PTN restored fetal weight in *Nfil3*<sup>-/-</sup> mice (Figures S8J and S8K). Taken together, these results confirm that induced CD49a<sup>+</sup> uterus-like NK cells could rebuild the local microenvironment for fetal development in the uterus and ameliorate the effects of FGR-mediated diseases in a GPF-dependent manner.

## DISCUSSION

The placenta which nourishes the fetus during mammalian pregnancy takes 4 months to form (Parham and Moffett, 2013; Ahokas, 2008). During the first trimester of pregnancy, NK cells comprise approximately 70% of all the lymphocytes in the uterus but significantly decline after the placenta is formed. We investigated whether these transient NK cells participate in the early

optimization of maternal nourishment of the fetus development; the data presented here showed that a uterine trNK cell subset has specific functions in secreting GPFs, such as PTN and OGN, and promoting fetal growth in both humans and mice. PTN has been shown to be implicated in many processes such as endothelial cell properties during normal and pathological angiogenesis (Perez-Pinera et al., 2008), neurite growth during brain development (Rauvala, 1989), and the development and regeneration of bone and cartilage (Dreyfus et al., 1998). OGN is a proteoglycan (PG) in the small leucine-rich proteoglycan (SLRP) family, which has key roles in heart development (Sarwar et al., 2009) and regulates the thickness of collagen fibrils in skin and eye (Williamson et al., 2008). Both GPFs are critical for fetal development.

Decidual NK cells have complex heterogeneity and exist in various subsets during early pregnancy. We have previously shown a tissue-resident NK cell subset with a CD49a<sup>+</sup>CD49b<sup>-</sup> phenotype in mouse liver (Peng et al., 2013; Peng and Sun, 2017). This subset of NK cells do not express Eomes and is already included in ILC1s (Gasteiger and Rudensky, 2014). In contrast with CD49a<sup>+</sup> tissue-resident NK cells in other organs, uterine human CD49a<sup>+</sup>CD49b<sup>-</sup> NK cell subsets have two populations: one subset shows no expression of Eomes and composes only a small percentage in human deciduas (regarded as CD49a<sup>+</sup>Eomes<sup>-</sup> uterus ILC1s); the other subset surprisingly expresses Eomes, which is expressed in 85% of all the NK cells from the normal human deciduas during the first trimester (regarded as CD49a<sup>+</sup>Eomes<sup>+</sup> uterus trNK cells). This CD49a<sup>+</sup>Eomes<sup>+</sup> uterine NK cell subset was different from previously identified liver ILC1s for both transcription factor expressions and the function. Uterine trNK cells not only express Eomes, but also need the transcription factor Nfil3 but not T-bet. Mouse liver-based tissue-resident NK cells are strictly dependent on T-bet but neither on Eomes nor Nfil3 (Cortez et al., 2014; Seillet et al., 2014; Sojka et al., 2014). Mucosal group 1 ILCs express CD49a and require T-bet but not Eomes in their development (Gordon et al., 2012; Klose et al., 2014). It has also been reported that salivary gland NK cells have a CD49a<sup>+</sup>Eomes<sup>+</sup> subset (Cortez et al., 2016), but these salivary gland CD49a<sup>+</sup> NK cells co-express CD49b, which is distinct from our reported results.

The studies presented here also demonstrated that the capability of GPF secretion by the uterine trNK cell subset is promoted by the HLA-G-ILT2-KIR2DL4 axis. HLA-G has been reported to be important in protecting the fetus from maternal uterine natural

(B) Statistics calculated by the percentage and cell number of trNK cell subsets isolated from virgin uteruses and deciduas at gestation day 6.5, 11.5, 15.5 of aged mice and control mice. Unpaired t test.

(C) Flow cytometry of GPFs and Eomes expressions in CD49a<sup>+</sup>NK1.1<sup>+</sup>CD3<sup>-</sup>CD19<sup>-</sup>CD45<sup>+</sup> dNK cells from WT mice and aged mice at gd10.5.

(D) Statistics calculated by the percentage of each GPF<sup>+</sup>Eomes<sup>+</sup> subset from CD49a<sup>+</sup> dNK cells from WT mice and aged mice. n = 5, unpaired t test.

(E) Quantitative RT-PCR of GPFs genes in virgin uterus from WT mice and aged mice. Data are representative of two independent experiments. Unpaired t test.

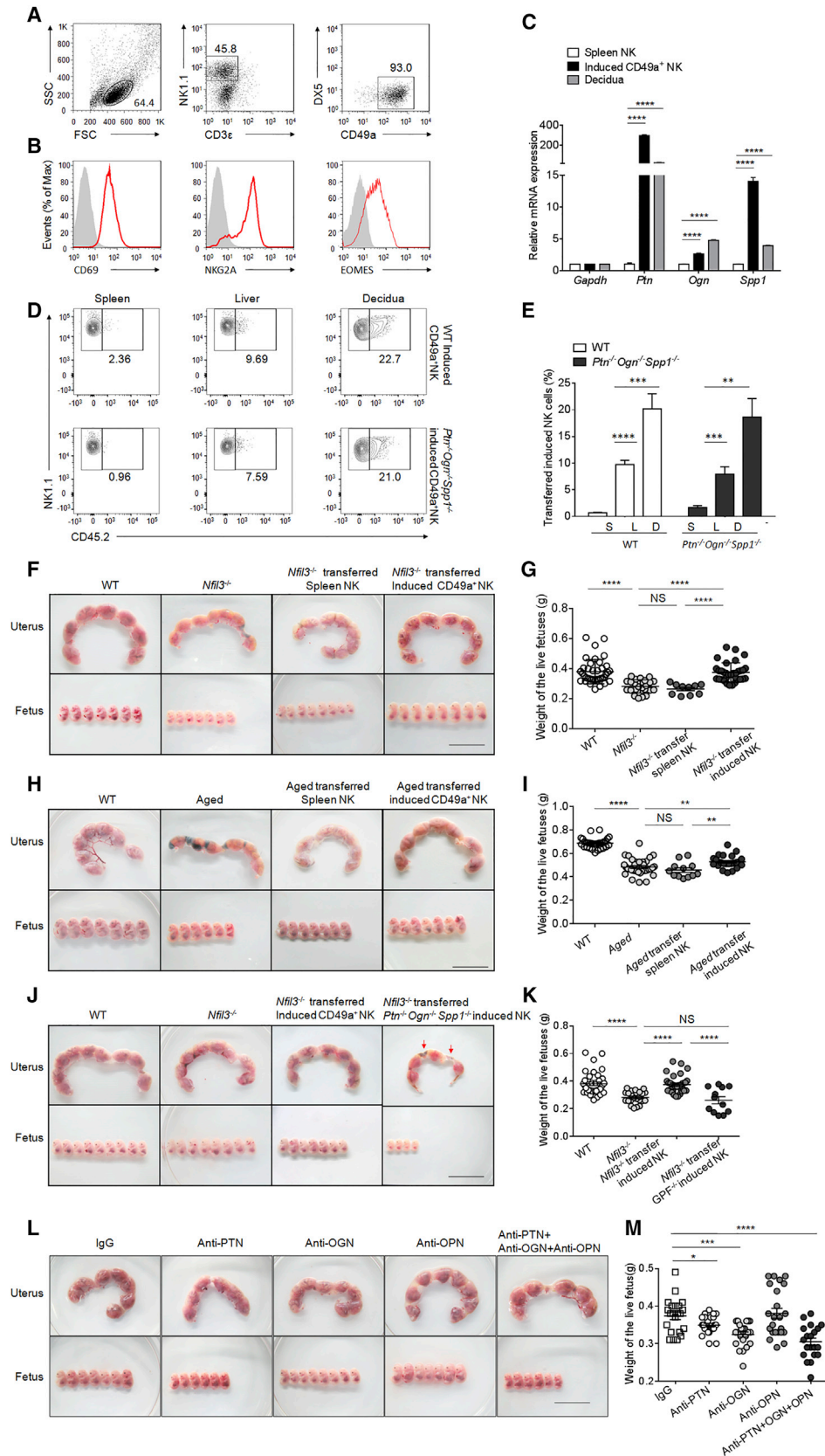
(F) Representative pictures of uteruses and fetuses from pregnant aged mice (aged female mated B6 male) and control mice (B6 female mated B6 male) at gd16.5. Bar: 3 cm. Data are representative of two independent experiments.

(G and H) Statistics calculated by the weight of uterus (n = 5, 7, respectively) and live fetus (n = 37, 40, respectively) in pregnant control mice and aged mice at gd16.5. Unpaired t test.

(I) Stereomicroscope representative pictures of fetal skeletal staining of embryos from pregnant aged mice (aged B6 female mated B6 male) and control mice (B6 female mated B6 male) at gd16.5. Bar: 1 mm.

(J) Von Kossa staining of skulls from control and aged group at gd16.5. Bars: 200 μm.

The numbers in (A) and (C) show the percentage of each indicated NK cell subset. Mean ± SEM, \*p < 0.05, \*\*p < 0.01, \*\*\*p < 0.005, \*\*\*\*p < 0.0001. See also Figure S5.



(legend on next page)

killer cytotoxicity (Rouas-Freiss et al., 1997), promoting vascular adaptations (Rajagopalan, 2014), and providing immune tolerance (Hunt et al., 2005) during pregnancy. The results presented in this study confirm that the low HLA-G expression determined by either an embryo or EVT is closely related with fetal disease. Blocking the HLA-G-ILT2-KIR2DL4 axis impeded the function of NK cells in secreting GPFs. It is still unclear whether these GPFs exert a direct effect toward fetal development. One possibility is that GPFs cross the maternal-fetal barrier and can directly affect the fetus. Another possibility is that GPFs exert an indirect effect by promoting placentation and vascularization.

Immunosenescence of NK cells is important in age-related hyporesponsiveness and pathologies (Camous et al., 2012). Pregnancy in old female mice is associated with severe developmental variability, including growth retardations, developmental delays, and impaired decidualization (Woods et al., 2017). Here we showed that aging also affects growth factor production from uterine trNK cells, a mechanism that is not fully understood. On the one hand, intrinsically programmed events in these uterine trNK cells may be operative, which would presume that these cells have some sort of internal clock that limits their function. Transcriptional and epigenetic regulations have been reported to vary in aging models and are subjected to functional alterations by reactive oxygen species (ROS) (Roy et al., 2002). On the other hand, a decline in the uterine microenvironment has been implicated in decreased growth factor secretion of trNK cells. In addition, the production of inflammatory mediators that increase with age (Michaud et al., 2013) may be interfering and transforming the function of uterus NK cells.

In the present study, it was demonstrated that adoptive transfer of these uterus-like NK cells reversed impaired fetal

growth and rebuilt the appropriate local microenvironment. Cytotoxic NK cell-based immunotherapy has been widely used to treat malignant diseases (El Costa et al., 2009; Cheng et al., 2013). However, as NK cells have complex heterogeneity, other subsets of NK cells with functional specialties have not been used as immunotherapies to date. The adoptive transfer of induced uterus-like NK cells as a cell treatment for FGR fetuses has many advantages. Similar to terminally differentiated cells, induced uterus-like NK cells are a much safer alternative than pluripotent stem cells. These uterus-like NK cells can be induced from expanded autologous or allogeneic NK cells as well as from umbilical cord blood stem cells. Intravenous infusion or administration via vaginal suppository to mothers without the use of an invasive procedure for both the mother and fetus is easier for patients to accept. Additional studies are needed to explore the most suitable protocols to induce uterus-like GPF-secreting NK cells in a human system and improve the feasibility of applying these uterus-like trNK cells to patients.

## STAR★METHODS

Detailed methods are provided in the online version of this paper and include the following:

- KEY RESOURCES TABLE
- CONTACT FOR REAGENT AND RESOURCE SHARING
- EXPERIMENTAL MODEL AND SUBJECT DETAILS
  - Human samples
  - Mice
  - Generation of the *Ptn*<sup>-/-</sup>*Ogn*<sup>-/-</sup>*Spp1*<sup>-/-</sup> mice
  - Cell Lines

### Figure 6. Adoptive Transfer-Induced CD49a<sup>+</sup> Uterus-like NK Cells Exhibit Rescue of FGR through GPFs

(A) Representative density plots showing the high CD49a expressions on the induced uterus-like NK cells. Data are representative of three independent experiments.

(B) Flow cytometry analysis of CD69, NKG2A, and Eomes expressions on the induced NK1.1<sup>+</sup> uterus-like NK cells.

(C) Quantitative RT-PCR of GPF genes in purified spleen NK cells, the induced uterus-like NK cells, and normal decidua tissues from B6 mice at gd15.5, normalized to their expressions in spleen NK cells alone. Data are representative of two independent experiments. Unpaired t test.

(D) Representative density plots showing NK1.1 and CD45.2 expression in CD45<sup>+</sup>NK1.1<sup>+</sup>CD3<sup>-</sup> NK cells from spleen, liver, and uterus of recipient CD45.1 mice. Induced uterus-like NK cells from the bone marrow of CD45.2 WT mice or *Ptn*<sup>-/-</sup>*Ogn*<sup>-/-</sup>*Spp1*<sup>-/-</sup> mice were purified and then injected via the tail vein into pregnant CD45.1 females on day 6.5 of gestation ( $1 \times 10^6$ /mouse). After 14 hr, the pregnant recipient mice were euthanized and the spleen, liver, and uterus were examined. Data are representative of two independent experiments.

(E) Statistics calculated by the percentage of the transferred CD45.2<sup>+</sup> NK cells in all NK cells of each spleen (S), liver (L), and decidua (D) from recipient mice. n = 4–5.

(F–I) Induced uterus-like NK cells were purified and then injected via the tail vein into pregnant *Nfil3*<sup>-/-</sup> or aged females on day 6.5 of gestation ( $1 \times 10^6$ /mouse). The pregnant recipient mice of each group were euthanized and the uterus were examined on gd15.5 (*Nfil3*<sup>-/-</sup> group) or gd16.5 (aged group).

(F) Representative pictures of uteruses and fetuses from pregnant WT mice, pregnant *Nfil3*<sup>-/-</sup> mice, and pregnant *Nfil3*<sup>-/-</sup> mice transferred induced CD49a<sup>+</sup> uterus-like NK cells or purified NK cells from spleen. Bars: 3 cm. Statistics calculated by the weight of live fetus. Data are representative of two independent experiments.

(G) Statistics calculated by the weight of live fetuses on gd15.5 of each group in (F). n = 38, 23, 10, 33, respectively. Unpaired t test.

(H) Representative pictures of uteruses and fetuses from pregnant WT mice, pregnant aged mice, and pregnant aged mice transferred induced CD49a<sup>+</sup> uterus-like NK cells or purified NK cells from spleen. Bars: 3 cm. Data are representative of two independent experiments.

(I) Statistics calculated by the weight of live fetus on gd16.5 of each group in (H). n = 30, 35, 12, 24, respectively. Unpaired t test.

(J and K) Induced uterus-like NK cells from B6 WT mice or *Ptn*<sup>-/-</sup>*Ogn*<sup>-/-</sup>*Spp1*<sup>-/-</sup> mice were purified and then injected via the tail vein into pregnant *Nfil3*<sup>-/-</sup> females on day 6.5 of gestation ( $1 \times 10^6$ /mouse). On gd15.5, the pregnant recipient mice of each group were examined.

(J) Representative pictures of uteruses and fetuses from pregnant *Nfil3*<sup>-/-</sup> mice transferred induced CD49a<sup>+</sup> uterus-like NK cells from WT mice or *Ptn*<sup>-/-</sup>*Ogn*<sup>-/-</sup>*Spp1*<sup>-/-</sup> mice. Bars: 3 cm. Data are representative of two independent experiments.

(K) Statistics calculated by the weight of live fetus in normal induced NK cells transferring group and *Ptn*<sup>-/-</sup>*Ogn*<sup>-/-</sup>*Spp1*<sup>-/-</sup> NK cells transferring group. n = 38, 23, 33, 12, respectively. Unpaired t test.

(L) Pictures of uteruses and fetuses from pregnant WT mice injected blocking antibodies of GPFs or IgG controls. Antibodies were injected via the tail vein into pregnant B6 mice on day 3.5, 6.5, and 10.5 of gestation (anti-PTN 5  $\mu$ g/200  $\mu$ L PBS, anti-OGN 5  $\mu$ g/200  $\mu$ L PBS, anti-OPN 5  $\mu$ g/200  $\mu$ L PBS for each injection).

(M) Statistics calculated by the weight of live fetus in B6 mice injected with GPF antibodies or IgG controls. n = 22, 25, 22, 23, 20, respectively. Unpaired t test. The numbers in (A) and (D) show the percentage of each indicated subset. Mean  $\pm$  SEM, \*p < 0.05, \*\*p < 0.01, \*\*\*p < 0.005, \*\*\*\*p < 0.0001. See also Figure S6.

## ● METHOD DETAILS

- Human samples isolation
- Quantitative PCR analysis of GPFs
- siRNA interfering of KIR2DL4 expressions
- Flow cytometry
- Immunofluorescence
- Skeletal and histological analysis
- Von Kossa staining
- Coculture system with 721.221-HLA-G
- Induced uterus-like NK cells *in vitro*
- Adoptive transfer of uterus-like NK cells
- Quantitation of fetus weight

## ● QUANTIFICATION AND STATISTICAL ANALYSIS

## ● DATA AND SOFTWARE AVAILABILITY

## SUPPLEMENTAL INFORMATION

Supplemental Information includes six figures and one table and can be found with this article online at <https://doi.org/10.1016/j.immuni.2017.11.018>.

## AUTHOR CONTRIBUTIONS

B.F. designed and performed the experiments and analyzed and interpreted the data. Y.Z. performed the experiments and constructed the *Ptn<sup>-/-</sup>Ogn<sup>-/-</sup>Spp1<sup>-/-</sup>* mice. X.N. constructed the *in vitro* system of induced uterus-like NK cells. R.S. established techniques of FACS and immunohistochemistry and interpreted the data. Z.D. assisted with data interpretation. X.T. and X.X. collected tissue samples and information from patients. Z.T. provided strategic planning, conceived the project, and interpreted some data. H.W. supervised the project, provided crucial ideas, and assisted with data interpretation. B.F. wrote the manuscript with H.W.

## ACKNOWLEDGMENTS

This work was supported by the Natural Science Foundation of China (91442202, 81788104, 81330071, and 81471527).

Received: April 4, 2017

Revised: September 1, 2017

Accepted: November 21, 2017

Published: December 19, 2017

## REFERENCES

- Ahokas, R., and McKinney, E. (2008). Development and physiology of the placenta and membranes. <https://doi.org/10.3843/GLOWM.10101>.
- Arck, P.C., and Hecher, K. (2013). Fetomaternal immune cross-talk and its consequences for maternal and offspring's health. *Nat. Med.* **19**, 548–556.
- Barber, E.M., and Pollard, J.W. (2003). The uterine NK cell population requires IL-15 but these cells are not required for pregnancy nor the resolution of a *Listeria monocytogenes* infection. *J. Immunol.* **171**, 37–46.
- Boulenouar, S., Doisne, J.M., Sferruzzi-Perri, A., Gaynor, L.M., Kieckbusch, J., Balmas, E., Yung, H.W., Javadzadeh, S., Volmer, L., Hawkes, D.A., et al. (2016). The residual innate lymphoid cells in NFIL3-deficient mice support suboptimal maternal adaptations to pregnancy. *Front. Immunol.* **7**, 43.
- Camous, X., Pera, A., Solana, R., and Larbi, A. (2012). NK cells in healthy aging and age-associated diseases. *J. Biomed. Biotechnol.* **2012**, 195956.
- Cheng, M., Chen, Y.Y., Xiao, W.H., Sun, R., and Tian, Z.G. (2013). NK cell-based immunotherapy for malignant diseases. *Cell Mol. Immunol.* **10**, 230–252.
- Choi, S.T., Kim, J.H., Kang, E.J., Lee, S.W., Park, M.C., Park, Y.B., and Lee, S.K. (2008). Osteopontin might be involved in bone remodeling rather than in inflammation in ankylosing spondylitis. *Rheumatology (Oxford)* **47**, 1775–1779.
- Colucci, F., and Kieckbusch, J. (2015). Maternal uterine natural killer cells nurture fetal growth: in medio stat virtus. *Trends Mol. Med.* **21**, 60–67.
- Cong, L., and Zhang, F. (2015). Genome engineering using CRISPR-Cas9 system. *Methods Mol. Biol.* **1239**, 197–217.
- Cortez, V.S., Cervantes-Barragan, L., Robinette, M.L., Bando, J.K., Wang, Y.M., Geiger, T.L., Gilfillan, S., Fuchs, A., Vivier, E., Sun, J.C., et al. (2016). Transforming Growth Factor-beta signaling guides the differentiation of innate lymphoid cells in salivary glands. *Immunity* **44**, 1127–1139.
- Cortez, V.S., Fuchs, A., Cella, M., Gilfillan, S., and Colonna, M. (2014). Cutting edge: Salivary gland NK cells develop independently of Nfil3 in steady-state. *J. Immunol.* **192**, 4487–4491.
- Doisne, J.M., Balmas, E., Boulenouar, S., Gaynor, L.M., Kieckbusch, J., Gardner, L., Hawkes, D.A., Barbara, C.F., Sharkey, A.M., Brady, H.J., et al. (2015). Composition, development, and function of uterine innate lymphoid cells. *J. Immunol.* **195**, 3937–3945.
- Dreyfus, J., Brunet-de Carvalho, N., Duprez, D., Raulais, D., and Vigny, M. (1998). HB-GAM/pleiotrophin: localization of mRNA and protein in the chicken developing leg. *Int. J. Dev. Biol.* **42**, 189–198.
- Eberl, G., Di Santo, J.P., and Vivier, E. (2015). The brave new world of innate lymphoid cells. *Nat. Immunol.* **16**, 1–5.
- El Costa, H., Tabiasco, J., Berrebi, A., Parant, O., Aguerre-Girr, M., Piccinni, M.P., and Le Bouteiller, P. (2009). Effector functions of human decidual NK cells in healthy early pregnancy are dependent on the specific engagement of natural cytotoxicity receptors. *J. Reprod. Immunol.* **82**, 142–147.
- Fu, B., Li, X., Sun, R., Tong, X., Ling, B., Tian, Z., and Wei, H. (2013). Natural killer cells promote immune tolerance by regulating inflammatory TH17 cells at the human maternal-fetal interface. *Proc. Natl. Acad. Sci. USA* **110**, E231–E240.
- Fu, B., Tian, Z., and Wei, H. (2014a). Subsets of human natural killer cells and their regulatory effects. *Immunology* **141**, 483–489.
- Fu, B.Q., Tian, Z.G., and Wei, H.M. (2014b). TH17 cells in human recurrent pregnancy loss and pre-eclampsia. *Cell Mol. Immunol.* **11**, 564–570.
- Fu, B., Wang, F., Sun, R., Ling, B., Tian, Z., and Wei, H. (2011). CD11b and CD27 reflect distinct population and functional specialization in human natural killer cells. *Immunology* **133**, 350–359.
- Gasteiger, G., and Rudensky, A.Y. (2014). Interactions between innate and adaptive lymphocytes. *Nat. Rev. Immunol.* **14**, 631–639.
- Gordon, S.M., Chaix, J., Rupp, L.J., Wu, J., Madera, S., Sun, J.C., Lindsten, T., and Reiner, S.L. (2012). The transcription factors T-bet and Eomes control key checkpoints of natural killer cell maturation. *Immunity* **36**, 55–67.
- Hanna, J., Goldman-Wohl, D., Hamani, Y., Avraham, I., Greenfield, C., Natanson-Yaron, S., Prus, D., Cohen-Daniel, L., Arnon, T.I., Manaster, I., et al. (2006). Decidual NK cells regulate key developmental processes at the human fetal-maternal interface. *Nat. Med.* **12**, 1065–1074.
- Hiby, S.E., Apps, R., Chazara, O., Farrell, L.E., Magnus, P., Trogstad, L., Gjessing, H.K., Carrington, M., and Moffett, A. (2014). Maternal KIR in combination with paternal HLA-C2 regulate human birth weight. *J. Immunol.* **192**, 5069–5073.
- Hiby, S.E., Apps, R., Sharkey, A.M., Farrell, L.E., Gardner, L., Mulder, A., Claas, F.H., Walker, J.J., Redman, C.W., Morgan, L., et al. (2010). Maternal activating KIRs protect against human reproductive failure mediated by fetal HLA-C2. *J. Clin. Invest.* **120**, 4102–4110.
- Hunt, J.S., Petroff, M.G., McIntire, R.H., and Ober, C. (2005). HLA-G and immune tolerance in pregnancy. *FASEB J.* **19**, 681–693.
- Jabrane-Ferrat, N., and Siewiera, J. (2014). The up side of decidual natural killer cells: new developments in immunology of pregnancy. *Immunology* **141**, 490–497.
- Jolly, M., Sebire, N., Harris, J., Robinson, S., and Regan, L. (2000). The risks associated with pregnancy in women aged 35 years or older. *Hum. Reprod.* **15**, 2433–2437.

- Juriscovica, A., Casper, R.F., MacLusky, N.J., Mills, G.B., and Librach, C.L. (1996). HLA-G expression during preimplantation human embryo development. *Proc. Natl. Acad. Sci. USA* **93**, 161–165.
- Kalkunte, S.S., Mselle, T.F., Norris, W.E., Wira, C.R., Sentman, C.L., and Sharma, S. (2009). Vascular endothelial growth factor C facilitates immune tolerance and endothelial activity of human uterine NK cells at the maternal-fetal interface. *J. Immunol.* **182**, 4085–4092.
- Kieckbusch, J., Gaynor, L.M., Moffett, A., and Colucci, F. (2014). MHC-dependent inhibition of uterine NK cells impedes fetal growth and decidual vascular remodelling. *Nat. Commun.* **5**, 3359.
- Klose, C.S., Flach, M., Mohle, L., Rogell, L., Hoyler, T., Ebert, K., Fabiunke, C., Pfeifer, D., Sexl, V., Fonseca-Pereira, D., et al. (2014). Differentiation of type 1 ILCs from a common progenitor to all helper-like innate lymphoid cell lineages. *Cell* **157**, 340–356.
- Koopman, L.A., Kopcow, H.D., Rybalov, B., Boyson, J.E., Orange, J.S., Schatz, F., Masch, R., Lockwood, C.J., Schachter, A.D., Park, P.J., and Strominger, J.L. (2003). Human decidual natural killer cells are a unique NK cell subset with immunomodulatory potential. *J. Exp. Med.* **198**, 1201–1212.
- Lash, G.E., Schiessl, B., Kirkley, M., Innes, B.A., Cooper, A., Searle, R.F., Robson, S.C., and Bulmer, J.N. (2006). Expression of angiogenic growth factors by uterine natural killer cells during early pregnancy. *J. Leukoc. Biol.* **80**, 572–580.
- LeMaout, J., Zafaranloo, K., Le Danff, C., and Carosella, E.D. (2005). HLA-G up-regulates ILT2, ILT3, ILT4, and KIR2DL4 in antigen presenting cells, NK cells, and T cells. *Faseb. J.* **19**, 662–664.
- Male, V., Sharkey, A., Masters, L., Kennedy, P.R., Farrell, L.E., and Moffett, A. (2011). The effect of pregnancy on the uterine NK cell KIR repertoire. *Eur. J. Immunol.* **41**, 3017–3027.
- Mansell, T., Novakovic, B., Meyer, B., Rzehak, P., Vuillermin, P., Ponsonby, A.L., Collier, F., Burgner, D., Saffery, R., and Ryan, J. (2016). The effects of maternal anxiety during pregnancy on IGF2/H19 methylation in cord blood. *Transl. Psychiatry* **6**, e765.
- Michaud, M., Balaray, L., Moulis, G., Gaudin, C., Peyrot, C., Vellas, B., Cesari, M., and Nourhashemi, F. (2013). Proinflammatory cytokines, aging, and age-related diseases. *J. Am. Med. Dir. Assoc.* **14**, 877–882.
- Nagashima, T., Li, Q., Clementi, C., Lydon, J.P., DeMayo, F.J., and Matzuk, M.M. (2013). BMPR2 is required for postimplantation uterine function and pregnancy maintenance. *J. Clin. Invest.* **123**, 2539–2550.
- Niu, Y., Shen, B., Cui, Y., Chen, Y., Wang, J., Wang, L., Kang, Y., Zhao, X., Si, W., Li, W., et al. (2014). Generation of gene-modified cynomolgus monkey via Cas9/RNA-mediated gene targeting in one-cell embryos. *Cell* **156**, 836–843.
- Otto, F., Thornell, A.P., Crompton, T., Denzel, A., Gilmour, K.C., Rosewell, I.R., Stamp, G.W., Beddington, R.S., Mundlos, S., Olsen, B.R., et al. (1997). *Cbfa1*, a candidate gene for cleidocranial dysplasia syndrome, is essential for osteoblast differentiation and bone development. *Cell* **89**, 765–771.
- Parham, P., and Moffett, A. (2013). Variable NK cell receptors and their MHC class I ligands in immunity, reproduction and human evolution. *Nat. Rev. Immunol.* **13**, 133–144.
- Peng, H., and Sun, R. (2017). Liver-resident NK cells and their potential functions. *Cell Mol. Immunol.* **14**, 890–894.
- Peng, H., Jiang, X., Chen, Y., Sojka, D.K., Wei, H., Gao, X., Sun, R., Yokoyama, W.M., and Tian, Z. (2013). Liver-resident NK cells confer adaptive immunity in skin-contact inflammation. *J. Clin. Invest.* **123**, 1444–1456.
- Perez-Pinera, P., Berenson, J.R., and Deuel, T.F. (2008). Pleiotrophin, a multifunctional angiogenic factor: mechanisms and pathways in normal and pathological angiogenesis. *Curr. Opin. Hematol.* **15**, 210–214.
- Rajagopalan, S. (2014). HLA-G-mediated NK cell senescence promotes vascular remodeling: implications for reproduction. *Cell Mol. Immunol.* **11**, 460–466.
- Rajagopalan, S., and Long, E.O. (2012). Cellular senescence induced by CD158d reprograms natural killer cells to promote vascular remodeling. *Proc. Natl. Acad. Sci. USA* **109**, 20596–20601.
- Rauvala, H. (1989). An 18-kd heparin-binding protein of developing brain that is distinct from fibroblast growth factors. *EMBO J.* **8**, 2933–2941.
- Rouas-Freiss, N., Gonçalves, R.M., Menier, C., Dausset, J., and Carosella, E.D. (1997). Direct evidence to support the role of HLA-G in protecting the fetus from maternal uterine natural killer cytotoxicity. *Proc. Natl. Acad. Sci. USA* **94**, 11520–11525.
- Roy, A.K., Oh, T., Rivera, O., Mubiru, J., Song, C.S., and Chatterjee, B. (2002). Impacts of transcriptional regulation on aging and senescence. *Ageing Res. Rev.* **1**, 367–380.
- Sanders, S.K., Giblin, P.A., and Kavathas, P. (1991). Cell-cell adhesion mediated by Cd8 and human histocompatibility leukocyte antigen-G, a nonclassical major histocompatibility complex class-1 molecule on cytotrophoblasts. *J. Exp. Med.* **174**, 737–740.
- Sarwar, R., Petretto, E., Grieve, I.C., Lu, H., Kumaran, M.K., Muckett, P.J., Mangion, J., Schroen, B., Benson, M., Punjabi, P.P., et al. (2009). Integrated genomics approaches identify osteoglycin as a regulator of left ventricular mass. *Heart* **95**, A4.
- Schulkey, C.E., Regmi, S.D., Magnan, R.A., Danzo, M.T., Luther, H., Hutchinson, A.K., Panzer, A.A., Grady, M.M., Wilson, D.B., and Jay, P.Y. (2015). The maternal-age-associated risk of congenital heart disease is modifiable. *Nature* **520**, 230–233.
- Seillet, C., Huntington, N.D., Gangatirkar, P., Axelsson, E., Minnich, M., Brady, H.J.M., Busslinger, M., Smyth, M.J., Belz, G.T., and Carotta, S. (2014). Differential requirement for Nfil3 during NK cell development. *J. Immunol.* **192**, 2667–2676.
- Singh, M., Dalal, S., and Singh, K. (2014). Osteopontin: At the cross-roads of myocyte survival and myocardial function. *Life Sci.* **118**, 1–6.
- Sojka, D.K., Plougastel-Douglas, B., Yang, L., Pak-Wittel, M.A., Artyomov, M.N., Ivanova, Y., Zhong, C., Chase, J.M., Rothman, P.B., Yu, J., et al. (2014). Tissue-resident natural killer (NK) cells are cell lineages distinct from thymic and conventional splenic NK cells. *eLife* **3**, e01659.
- Sun, L.L., Wang, A.M., Haines, C.J., Han, Y., and Yao, Y.Q. (2011). Down-regulation of HLA-G attenuates cleavage rate in human triploid embryos. *J. Reprod. Infertil.* **12**, 215–220.
- Tilburgs, T., Evans, J.H., Crespo, A.C., and Strominger, J.L. (2015). The HLA-G cycle provides for both NK tolerance and immunity at the maternal-fetal interface. *Proc. Natl. Acad. Sci. USA* **112**, 13312–13317.
- Vacca, P., Mingari, M.C., and Moretta, L. (2013). Natural killer cells in human pregnancy. *J. Reprod. Immunol.* **97**, 14–19.
- Wang, H., Yang, H., Shivalila, C.S., Dawlaty, M.M., Cheng, A.W., Zhang, F., and Jaenisch, R. (2013). One-step generation of mice carrying mutations in multiple genes by CRISPR/Cas-mediated genome engineering. *Cell* **153**, 910–918.
- Williamson, R.E., Darrow, K.N., Giersch, A.B.S., Resendes, B.L., Huang, M., Conrad, G.W., Chen, Z.Y., Liberman, M.C., Morton, C.C., and Tasheva, E.S. (2008). Expression studies of osteoglycin/mimecan (OGN) in the cochlea and auditory phenotype of Ogn-deficient mice. *Hear. Res.* **237**, 57–65.
- Woods, L., Perez-Garcia, V., Kieckbusch, J., Wang, X., DeMayo, F., Colucci, F., and Hemberger, M. (2017). Decidualisation and placentation defects are a major cause of age-related reproductive decline. *Nat. Commun.* **8**, 352.
- Xiong, S., Sharkey, A.M., Kennedy, P.R., Gardner, L., Farrell, L.E., Chazara, O., Bauer, J., Hiby, S.E., Colucci, F., and Moffett, A. (2013). Maternal uterine NK cell-activating receptor KIR2DS1 enhances placentation. *J. Clin. Invest.* **123**, 4264–4272.
- Zhang, J., Chen, Z., Smith, G.N., and Croy, B.A. (2011). Natural killer cell-triggered vascular transformation: maternal care before birth? *Cell Mol. Immunol.* **8**, 1–11.
- Zhang, J.H., Dunk, C.E., Kwan, M., Jones, R.L., Harris, L.K., Keating, S., and Lye, S.J. (2017). Human dNK cell function is differentially regulated by extrinsic cellular engagement and intrinsic activating receptors in first and second trimester pregnancy. *Cell Mol. Immunol.* **14**, 203–213.

## STAR★METHODS

## KEY RESOURCES TABLE

REAGENT or RESOURCE	SOURCE	IDENTIFIER
Antibodies		
Anti-human CD3 PerCP-Cy5.5	BD	Cat#340949; RRID: AB_400190
Anti-human CD3 PerCP-Cy5.5	eBioscience	Cat#45-0036-42; RRID: AB_1518742
Anti-human CD3 PerCP-Cy5.5	Biolegend	Cat#300328; RRID: AB_1575008
Anti-human CD3 APC-Cy7	BD	Cat#557832; RRID: AB_396890
Anti-human CD3 BV 605	Biolegend	Cat#344836; RRID: AB_2565825
Anti-human CD8 FITC	BD	Cat#555366; RRID: AB_395769
Anti-human CD8 Alexa Fluor 700	Biolegend	Cat#344724; RRID: AB_2562790
Anti-human CD9 PE	Biolegend	Cat#312105; RRID: AB_2075893
Anti-human CD11b Alexa Fluor 488	BD	Cat#557701; RRID: AB_2129268
Anti-human CD11b PE-CY7	BD	Cat#557743; RRID: AB_396849
Anti-human CD16 FITC	BD	Cat#555406; RRID: AB_395806
Anti-human CD27 FITC	BD	Cat#555440; RRID: AB_395833
Anti-human CD27 PE	BD	Cat#555441; RRID: AB_395834
Anti-human CD27 PerCP-Cy5.5	BD	Cat#560612; RRID: AB_1727457
Anti-human CD45 PE	BD	Cat#555483; RRID: AB_395875
Anti-human CD45 BV 570	Biolegend	Cat#304033; RRID: AB_10899568
Anti-human CD49a Alexa Fluor 647	Biolegend	Cat#328310; RRID: AB_2129242
Anti-human CD49a PE-Cy7	Biolegend	Cat#328311; RRID: AB_2566271
Anti-human CD56 PE	BD	Cat#555516; RRID: AB_395906
Anti-human CD56 PE-Cy7	BD	Cat#557747; RRID: AB_396853
Anti-human CD56 Alexa Fluor 647	BD	Cat#557711; RRID: AB_396820
Anti-human CD56 Purified	Santa Cruz	Cat#sc-7326; RRID: AB_627127
Anti-human ILT2 PE-Cy7	Biolegend	Cat#333711; RRID: AB_2564605
Anti-human ILT2 Purified	Biolegend	Cat#333704; RRID: AB_1089088
Anti-human ILT4 PE	Biolegend	Cat#338705; RRID: AB_2136525
Anti-human ILT4 Purified	eBioscience	Cat#16-5148-81; RRID: AB_10670018
Anti-human EOMES FITC	eBioscience	Cat#11-4877-41; RRID: AB_2572498
Anti-human EOMES PE	eBioscience	Cat#12-4877-41; RRID: AB_2572614
Anti-human EOMES PerCP-eFluor 710	eBioscience	Cat#46-4877-41; RRID: AB_2573758
Anti-human T-bet PE	eBioscience	Cat#12-5825-82; RRID: AB_925761
Anti-human KIR2DL4 APC	Biolegend	Cat#347007; RRID: AB_2249479
Anti-human KIR2DL4 Purified	Biolegend	Cat#347003; RRID: AB_2028425
Anti-human HLA-G PE	Biolegend	Cat#335905; RRID: AB_1227710
Anti-human HLA-G Purified	Biolegend	Cat#335904; RRID: AB_10641840
Anti-human HLA-G Purified	Abcam	Cat#ab52454; RRID: AB_880554
Anti-human HLA-ABC PE	BD	Cat#560168; RRID: AB_1645510
Anti-human PTN Purified	LifeSpan	Cat#LS-C162291
Anti-human OGN Purified	LifeSpan	Cat#LS-B10948
Anti-human OPN Alexa Fluor 488	Abcam	Cat#ab196445
Anti-mouse CD3 $\epsilon$ PerCP-Cy5.5	Biolegend	Cat#100328; RRID: AB_893318
Anti-mouse CD3 $\epsilon$ APC-Cy7	Biolegend	Cat#100330; RRID: AB_1877170
Anti-mouse CD11b FITC	BD	Cat#553310; RRID: AB_394774
Anti-mouse CD11b PerCP-Cy5.5	Biolegend	Cat#101228; RRID: AB_893232
Anti-mouse CD19 APC-Cy7	Biolegend	Cat#115530; RRID: AB_830707

(Continued on next page)

**Continued**

REAGENT or RESOURCE	SOURCE	IDENTIFIER
Anti-mouse CD27 FITC	Biolegend	Cat#124208; RRID: AB_1236466
Anti-mouse CD27 PE	Biolegend	Cat#124210; RRID: AB_1236459
Anti-mouse CD45.2 PerCP-Cy5.5	Biolegend	Cat#109828; RRID: AB_893350
Anti-mouse CD49a PE	BD	Cat#562115; RRID: AB_11153117
Anti-mouse CD49a Alexa Fluor 647	BD	Cat#562113; RRID: AB_11153312
Anti-mouse CD49b FITC	BD	Cat#553857; RRID: AB_395093
Anti-mouse NKp46 PE	Biolegend	Cat#137604; RRID: AB_2235755
Anti-mouse NKp46 Alexa Fluor 647	eBioscience	Cat#51-3351-80; RRID: AB_1257146
Anti-mouse NK-1.1 PE-Cy7	Biolegend	Cat#108714; RRID: AB_389364
Anti-mouse Eomes Alexa Fluor 660	eBioscience	Cat#50-4875-82; RRID: AB_2574227
Anti-mouse T-bet PE	Biolegend	Cat#644810; RRID: AB_2200542
Anti-mouse PTN Purified	LifeSpan	Cat#LS-C295980
Anti-mouse PTN Purified	LifeSpan	Cat#LS-C387277
Anti-mouse OGN Purified	LifeSpan	Cat#LS-C387062
Anti-mouse OGN Purified	LifeSpan	Cat#LS-C295735
Anti-mouse OPN PE	LifeSpan	Cat#LS-C131160-100; RRID: AB_10832766
Anti-mouse OPN Purified	Abcam	Cat#ab91655; RRID: AB_2050147
Anti-mouse OPN Purified	R&D	Cat#AF808; RRID: AB_2194992
Mouse IgG <sub>1</sub> , κ FITC	BD	Cat#555748; RRID: AB_396090
Mouse IgG <sub>1</sub> , κ PE	BD	Cat#555749; RRID: AB_396091
Mouse IgG <sub>1</sub> , κ PerCP-Cy5.5	BD	Cat#552834; RRID: AB_394484
Mouse IgG <sub>1</sub> , κ PE-Cy7	BD	Cat#557872; RRID: AB_396914
Mouse IgG <sub>1</sub> , κ Alexa Fluor 647	BD	Cat#557714; RRID: AB_396823
Mouse IgG <sub>1</sub> , κ APC-Cy7	BD	Cat#557873; RRID: AB_396915
Mouse IgG <sub>1</sub> , κ Alexa Fluor 700	BD	Cat#557882; RRID: AB_396920
Mouse IgG <sub>1</sub> , κ BV 605	Biolegend	Cat#400161; RRID: AB_11125373
Mouse IgG <sub>2a</sub> , κ PE	BD	Cat#555574; RRID: AB_395953
Mouse IgG <sub>2a</sub> , κ PerCP-Cy5.5	BD	Cat#558020; RRID: AB_396989
Mouse IgG <sub>2b</sub> , κ PE-Cy7	Biolegend	Cat#400325
Rat IgG <sub>2a</sub> , κ PE	BD	Cat#555844; RRID: AB_396167
Rat IgG <sub>2a</sub> , κ Alexa Fluor 647	BD	Cat#557690; RRID: AB_396799
Rat IgG <sub>2a</sub> , κ Alexa Fluor 660	eBioscience	Cat#50-4321-80; RRID: AB_10598640
Rat IgG <sub>2a</sub> , κ APC-Cy7	Biolegend	Cat#400524
Rat IgM, κ FITC	Biolegend	Cat#400806; RRID: AB_326582
Rat IgG <sub>2b</sub> , κ PerCP-Cy5.5	BD	Cat#550764; RRID: AB_393874
Rat IgG <sub>2b</sub> , κ PE-Cy7	BD	Cat#552868; RRID: AB_394490
Hamster IgG FITC	Biolegend	Cat#400905
Hamster IgG PE	Biolegend	Cat#400907
Hamster IgG PerCP/Cy5.5	Biolegend	Cat#400931
Hamster IgG APC/Cy7	Biolegend	Cat#400927
Hamster IgG <sub>2,λ1</sub> PE	BD	Cat#553965; RRID: AB_395166
Hamster IgG <sub>2,λ1</sub> Alexa Fluor 647	BD	Cat#562112; RRID: AB_11153854
Rabbit IgG Purified	CST	Cat#2729S; RRID: AB_1031062
Goat Anti-Rabbit IgG FITC	BD	Cat#554020; RRID: AB_395212
Goat anti-Rabbit IgG (H+L) Alexa Fluor 488	Thermo Fisher Scientific	Cat#A-11008; RRID: AB_143165
Goat anti-Rabbit IgG (H+L) Alexa Fluor 647	Thermo Fisher Scientific	Cat#A-32733; RRID: AB_2633282
Goat anti-Mouse IgG (H+L) Alexa Fluor 546	Thermo Fisher Scientific	Cat#A-11030; RRID: AB_144695

(Continued on next page)

**Continued**

REAGENT or RESOURCE	SOURCE	IDENTIFIER
Chemicals, Peptides, and Recombinant Proteins		
Recombinant Mouse PTN	R&D	Cat#6580-PL-050
Recombinant Mouse OGN	R&D	Cat#2949-MC-050
Recombinant Mouse OPN	R&D	Cat#441-OP-050/CF
Recombinant Mouse SCF	PeptoTech	Cat#250-03
Recombinant Mouse Fit3L	PeptoTech	Cat#250-31L
Recombinant Mouse IL-7	PeptoTech	Cat#217-17
Recombinant Mouse IL-15	PeptoTech	Cat#210-15
Recombinant Mouse IL-4	PeptoTech	Cat#214-14
Recombinant Human IL-2	Jiangsu Kingsley Pharmaceutical Co.	Cat#S10970056
Recombinant Mouse IL-6	PeptoTech	Cat#216-16
Recombinant Mouse IL-3	PeptoTech	Cat#213-13
Critical Commercial Assays		
Human Gene Expression Array	Affymetrix	Cat#GSE24268
Anti-PE Microbeads	Miltenyi Biotec	Cat#130-048-801; RRID: AB_244373
NK cell Isolation Kit	Miltenyi Biotec	Cat#130-092-657
Nucleofector Kits for Human Natural Killer Cells	Lonza	Cat#VPA-1005
Electroporetic transfected Kit for 721.221	Lonza	Cat#VCA-1003
Deposited Data		
Microarray analysis in CD49a <sup>+</sup> NK and CD49a <sup>-</sup> NK cells	This paper	GEO: GSE97217
Oligonucleotides		
Primers for human <i>ACTB</i> (NM_001101.3), Forward: TGACGTGGACATCCGCAAGACC; Reverse: CTCAGGAGGAGCAATGATCTTGA	This paper	N/A
Primers for human <i>PTN</i> (NM_002825), Forward: CCTCCCTGTCAGGGCGTAAT; Reverse: GACGGATGACTCACTGGTCTCTTT	This paper	N/A
Primers for human <i>OGN</i> (NM_024416.4), Forward: GAGGATAAATACCTGGATGGA; Reverse: GTGCGTAAAGATAGGCTGATT	This paper	N/A
Primers for human <i>SPP1</i> (NM_000582), Forward: TGAGAGCAATGAGCATTCCGATG; Reverse: CAGGGAGTTTCCATGAAGCCAC	This paper	N/A
Primers for mouse <i>Gapdh</i> (NM_008084.3), Forward: TGCACCACCAACTGCTTAG; Reverse: GGATGCAGGGATGATGTTT	This paper	N/A
Primers for mouse <i>Ptn</i> (NM_008973.2), Forward: TGGAGAATGGCAGTGGAGTGT; Reverse: GGCGGTATTGAGGTCACATTC	This paper	N/A
Primers for mouse <i>Ogn</i> (NM_008760.4), Forward: TGCTTTGTGGTCACATGGAT; Reverse: GAAGCTGCACACAGCACAAT	This paper	N/A
Primers for mouse <i>Spp1</i> (NM_001204203.1), Forward: TTAGACTCAACGCTCTTCAT; Reverse: TTAGACTCAACGCTCTTCAT	This paper	N/A
siRNA targeting sequence: Negative Control UUCUCCGAACGUGUCACGUTT	GenePharma	Cat# A06001
siRNA targeting sequence: siKIR2DL4-1, GGUCUAUAUGAGAAACCUUUU	GenePharma	N/A
siRNA targeting sequence: siKIR2DL4-2, GAGCUCUACAACAGAAUAUUU	GenePharma	N/A
Software and Algorithms		
Paired sgRNA oligos design tool	Cong and Zhang (2015)	<a href="http://crispr.mit.edu/">http://crispr.mit.edu/</a>

## CONTACT FOR REAGENT AND RESOURCE SHARING

Further information and requests for resources and reagents should be directed to and will be fulfilled by the Lead Contact, Haiming Wei ([ustcwhm@ustc.edu.cn](mailto:ustcwhm@ustc.edu.cn)).

## EXPERIMENTAL MODEL AND SUBJECT DETAILS

### Human samples

Decidual samples from normal pregnancies (n = 43) were obtained from elective pregnancy terminations. Eleven deciduas from abnormal pregnancies were obtained from patients who experienced recurrent spontaneous abortions and had a normal embryo karyotype (Table S1). Chorionic villi were sampled from the aborted cells for cytogenetic analysis. Genetic or anatomical causes of the abortions were excluded. Before surgery, informed consent was obtained from each patient. The decidual samples were collected from patients at the Anhui Provincial Hospital. Echo sonography was performed every two weeks, and patients were advised to obtain an induced abortion if the fetal heartbeat was either never detected or ceased. Fetal heartbeat was identified before elective termination among women with a normally progressing pregnancy. None of the subjects had any risk factors such as genetic abnormalities (neither themselves nor their husbands), uterine malformation, thyroid dysfunction, anti-phospholipid antibody syndrome or severe inflammation. Twelve normal morulas and 39 abnormal morulas that presented non-integer cleavage were donated with informed consent by the patients treated at the Assisted Reproduction Department at the Anhui Provincial Hospital. Mononuclear cells from peripheral blood (Blood Center of Anhui Province) and cord blood (Anhui Provincial Hospital) were prepared from buffy coats obtained from healthy donors by centrifugation using a Ficoll system. Ethical approval was obtained from the Ethics Committee at the University of Science & Technology of China.

### Mice

Male and female C57BL/6 mice (8 to 12 weeks old) were purchased from the Shanghai Experimental Animal Center of the Chinese Academy of Science (Shanghai, China). The *Nfil3*<sup>-/-</sup> mice were a generous gift from Prof. Tak Wah Mak (University of Toronto, Canada). *Tbx21*<sup>-/-</sup> mice were obtained from the Jackson Laboratory. Aged female mice (11 to 14 months old) were purchased from the Experimental Animal Center of the University of Science & Technology of China. All animals were kept under specific pathogen-free conditions. All of the experimental procedures involving animals were conducted in accordance with the National Guidelines for Animal Usage in Research (China) and permission for these animal studies was obtained from the Ethics Committee at the University of Science & Technology of China. B6 males were randomly introduced to virgin mice and the timing of conception was determined by detection of a copulation plug as gd0.5.

### Generation of the *Ptn*<sup>-/-</sup>*Ogn*<sup>-/-</sup>*Spp1*<sup>-/-</sup> mice

*Ptn*<sup>-/-</sup>*Ogn*<sup>-/-</sup>*Spp1*<sup>-/-</sup> mice were generated using CRISPR-Cas9 technology according to previous reports (Niu et al., 2014; Wang et al., 2013). sgRNA was designed to separately targeting the genes of *Ptn*, *Ogn* and *Spp1*. Paired sgRNA oligos were designed by tools from the Zhang Lab, at MIT (<http://crispr.mit.edu>). Either BLAT or BLAST searches of the sgRNA target sites in UCSC or the ENSEMBL genome database were browsed to find sequences with few or no related sites in the genome. Oligos were then synthesized, annealed, and inserted into sgRNA expression vectors (pUC57-sgRNA plasmid Addgene 51132). Paired sgRNA plasmids were digested with Dra I and purified using a MinElute PCR Purification kit (QIAGEN, 28004). Transcription of the sgRNAs *in vitro* was performed using a MEGAscript kit (Ambion, AM1354). Purifying the sgRNAs was accomplished using a MEGAclear kit (Ambion, AM1908) according to the manufacturer's instructions. We digested the Cas9 plasmid pST1374-NLS-flag-linker-Cas9 (Addgene44758) with Age I and purified the digestion product *in vitro*, and transcribed Cas9 using an mMESSEmMACHINE® T7 Ultra kit (Ambion, AM1345) according to the manufacturer's instructions. The Cas9 mRNA was purified using an RNeasy Mini kit (QIAGEN, 74104). The yields of sgRNA and Cas9 mRNA were assessed using the One Drop OD-1000+ spectrophotometer. C57BL/6J mice zygotes were superovulated by injection with PMSG (5 IU/100  $\mu$ l) and HCG (5 IU/100  $\mu$ l). DEPC-treated water was used to dilute Cas9 mRNA to a concentration of 20ng/ $\mu$ l and the sgRNAs (5 ng/ $\mu$ l each, three sets of sgRNAs separately targeting the genes of *Ptn*, *Ogn* and *Spp1*) in a final volume of 50  $\mu$ l. Microinjection and embryo transferring were performed using standard methods to generate transgenic mice, as previously described (Niu et al., 2014; Wang et al., 2013). We injected the RNA mixture into both the cytoplasm and larger (male) pronucleus. The gene phenotype of the genetically ablated mice was analyzed by sequence analysis of the target genome segment (Figure S6).

### Cell Lines

The MHC class I negative human B cell line 721.221 was a female transformed cell line and a generous gift from Prof. Xiongwen Wu (Huazhong University of Science and Technology, China). Cells were cultured in a complete RPMI medium 1640 (GIBCO, Grand Island, NY, U.S.A.) with 10% fetal bovine serum (HyClone, Logan, UT, U.S.A.) plus 1% streptomycin and penicillin under 37°C.

## METHOD DETAILS

### Human samples isolation

Decidual sample isolation was performed according to our previous report (Fu et al., 2013). Briefly, fresh decidua samples were washed and minced into small pieces. Decidual lymphocytes were released by digesting the tissues with 1 mg/mL collagenase type IV (Sigma-Aldrich) and 0.01 mg/mL DNase I (Sigma-Aldrich) in RPMI 1640 medium for 40 min at 37°C. The suspensions were strained through nylon mesh and then loaded onto a Ficoll density gradient to purify the lymphocytes. Stromal cells and macrophages were excluded after the cells were allowed to adhere to the culture plates for 2 h at 37°C. Decidual lymphocytes were then immediately used for subsequent the flow cytometry analysis. For the NK functional assays, NK cells were further purified via negative selection with a magnetic-activated cell sorter (MACS) (Miltenyi Biotec). The purity of the resulting dNK population was greater than 92% CD56<sup>+</sup>CD3<sup>-</sup>CD14<sup>-</sup>. Sorting of CD49a<sup>+</sup>NK cells (gated by CD56<sup>+</sup>CD3<sup>-</sup>CD45<sup>+</sup>CD49<sup>+</sup>CD49b<sup>-</sup>) from the fresh deciduas from the first trimester and CD49a<sup>-</sup>NK cells (gated by CD56<sup>+</sup>CD3<sup>-</sup>CD45<sup>+</sup>CD49<sup>-</sup>CD49b<sup>+</sup>) from the peripheral blood of healthy donors was performed using a FACS Aria (BD Bioscience). The purity of these sorted populations was greater than 92% for CD56<sup>+</sup>CD3<sup>-</sup>CD14<sup>-</sup>. EVT cells were isolated as previously described (Tilburgs et al., 2015). Briefly, villous tissue was gently scraped from the basal membrane, and then the tissue was digested for 10 min at 37°C with trypsin (0.2%) and EDTA (0.02%). Trypsin was quenched with F12 medium containing 10% (vol/vol) newborn calf serum (GIBCO). Cells were filtered over a nylon mesh washed once with complete F12 medium and layered on a Ficoll gradient for density gradient centrifugation. The resulting cells were collected, washed once, and incubated for 20 min at 37°C in a tissue culture dish to remove the macrophages.

### Quantitative PCR analysis of GPFs

To compare the expression of GPFs in NK cells and uterus tissues, we extracted total RNA from purified human decidual NK cells and the uteruses of virgin B6, Nfil3<sup>-/-</sup> and aged mice. Total RNA was extracted using TRIzol reagent (Invitrogen) and reverse-transcribed using an oligo dT primer (Invitrogen). The resulting cDNA was analyzed for the expression of various GPFs, genes using real-time quantitative RT-PCR with SYBR Premix Ex Taq (Tli RNaseH Plus, TaKaRa) and the appropriate primers for target genes in human and mouse samples (KEY RESOURCES TABLE).

### SiRNA interfering of KIR2DL4 expressions

SiRNA-KIR2DL4-1/2 and siRNA-NC were electroporetically transfected into purified human decidual NK cells from normal pregnancies during the first trimester using a Nucleofector Kits for Human Natural Killer Cells (VPA-1005, Lonza). The transfected dNK cells were co-cultured with EVT cells for 48h, and then separated using anti-CD56 MACS sorting followed by further analysis for GPF expressions (KEY RESOURCES TABLE).

### Flow cytometry

Suspensions of lymphocytes were stained for the following human or mouse mAbs (KEY RESOURCES TABLE). Homologous ;IgGs were used as negative control Abs. FACS staining was performed according to the manufacturer's instructions (BD Biosciences). Data from 20,000–50,000 single-cell events were collected using a standard FACSCalibur flow cytometer (BD Biosciences). Figure S2 A-C was collected using Sony Spectral Analyzer SP6800Z. Intracellular staining of GPFs was performed on decidual cells with or without 4 h of stimulation with PMA (50 ng/mL; Sigma) and ionomycin (1 µg/mL; Calbiochem) in the presence of monensin (10 µg/mL; Sigma). The cells were then collected, washed, and blocked according to instructions of eBioscience (Foxp3 / Transcription Factor Staining Buffer Set, eBioscience). The antibody used for intracellular staining is also shown in KEY RESOURCES TABLE.

### Immunofluorescence

Decidual tissues were fixed with 4% PFA at 4°C overnight, protected in 30% sucrose for 24 h at 4°C and then embedded in OCT and finally snap frozen. NK cells from either PBMCs or deciduas were purified using MACS (NK Cell Isolation Kit, human; Miltenyi Biotec). The purified cells and the cryostat sections were fixed with 4%PFA and incubated in blocking buffer (5% normal goat serum, 0.5% Triton-X in PBS) at room temperature for 1 hour. Primary and secondary antibodies were added, followed by staining with DAPI. The following primary antibodies were used: anti-CD56 (mouse, 1:50, Santa Cruz Biotechnology, sc-7326), anti-mouse (goat, 1:200, Invitrogen, A-11030), anti-GPFs (1:50) and anti-rabbit (goat, 1:200, Invitrogen, A-11008). All immunofluorescence staining was performed in the dark. Normal and abnormal embryos were washed three times with PBS+0.1%BSA, and then fixed with 4% PFA at room temperature for 15 min. After being washed in PBS+0.1%BSA three times, cells were incubated in 1.0%Triton X-100 for 30 min and then 1%BSA for 1 hour. The cells were stained with primary and secondary antibodies, and then stained with DAPI. The antibodies used are shown in KEY RESOURCES TABLE.

### Skeletal and histological analysis

For the staining and visualization of whole skeletons at each gestation day, we stained cleared skeletons of embryos with Alizarin red S and Alcian blue as described (Otto et al., 1997). Embryos at gd14.5, 15.5, 16.5 and 18.5 were eviscerated and the skin was removed. After overnight fixation in 95% ethanol, embryos were stained in Alcian blue solution overnight, following several hours

in 95% ethanol. The embryos were then transferred to 1% KOH for approximately 24–48 hours, followed by overnight staining in Alizarin red solution. Skeletons were cleared in 1% KOH/ 20% glycerol and finally stored in 50% glycerol.

### Von Kossa staining

The paraffin sections from paraffin-embedded embryos were dewaxed in xylene and rehydrated with distilled water, then fixed in 4% PFA/0.1 M phosphate buffer, and sections (thickness: 7  $\mu$ m) were stained with hematoxylin, eosin and von Kossa as described (Otto et al., 1997).

### Coculture system with 721.221-HLA-G

HLA-G (Youbio, NM-002127) or HLA-C (Youbio, NM\_002117) or Control-eGFP was electroporetically transfected into 721.221 using cell lines kit V. (VCA-1003, lonza). After 12h of transfection, the 721.221-HLA-G cells and 721.221-HLA-C were screened by 1 $\mu$ g/ml puromycin for 1 week (Figure S2). After screening, the 721.221-HLA-G cells or 721.221-HLA-C or 721.221-Control were co-cultured with purified human decidual NK cells from normal first trimester pregnancy for 48h. Decidual NK cells were separated from the system by anti-CD56 MACS sorting and further analyzed for GFPs expressions.

### Induced uterus-like NK cells *in vitro*

In order to generate murine decidual NK cells from BM lineage<sup>-</sup> cells *in vitro*, B6 mice or *Ptn*<sup>-/-</sup>*Ogn*<sup>-/-</sup>*Spp1*<sup>-/-</sup> mice were treated intraperitoneally with 5-fluorouracil (Sigma) at 200mg/kg body weight. Four days later, bone marrow cells were collected and cultured in IMDM medium (10% fetal bovine serum, 2mM L-glutamine, 1% penicillin and streptomycin). Recombinant murine SCF (50ng/ml), IL-6 (10ng/ml), IL-3 (6ng/ml) (all from PeproTech) were used for hematopoietic progenitor cell (HPC) proliferation. On day 3, cultures were collected and lineage<sup>-</sup> cells were isolated using a lineage cell depletion kit (Miltenyi Biotec). Purified cells were cultured in IMDM medium and recombinant murine SCF (5ng/ml), Flt3L (5ng/ml), IL-7(5ng/ml), IL-15(30ng/ml), and IL-2 (200UI/ml) were used for supporting uterus-like NK cells generation. On day 30, cells were collected for analysis and further purified using PE-anti-NKp46 antibody and anti-PE microbeads (Miltenyi Biotec). The purity of these sorted populations was greater than 95% for NKp46<sup>+</sup>NK1.1<sup>+</sup>CD3<sup>-</sup>CD19<sup>-</sup>. These purified induced uterus-like NK cells were collected, washed and prepared for adoptive transfer.

### Adoptive transfer of uterus-like NK cells

B6 males were randomly introduced to virgin *Nfil3*<sup>-/-</sup> mice or aged mice, and the timing of detection of a copulation plug was regarded as gd0.5. The induced uterus-like NK cells from B6 mice or *Ptn*<sup>-/-</sup>*Ogn*<sup>-/-</sup>*Spp1*<sup>-/-</sup> mice were purified by MACS, and were suspended in 200  $\mu$ L of PBS and injected via the tail vein into pregnant *Nfil3*<sup>-/-</sup> or aged females on day 6.5 of gestation ( $1 \times 10^6$  /mouse). The spleen NK cells from B6 mice were purified by MACS, and were suspended in 200  $\mu$ L of PBS and injected via the tail vein into pregnant *Nfil3*<sup>-/-</sup> or aged females on day 6.5 of gestation ( $1 \times 10^6$  /mouse) as controls. On gd15.5, the pregnant *Nfil3*<sup>-/-</sup> recipient mice were euthanized. On gd16.5, the pregnant aged recipient mice were euthanized. The uteri were examined for fetus weights.

### Quantitation of fetus weight

On gd15.5, gd16.5 and gd18.5, the pregnant mice of each group were euthanized, and the uteri were examined for the fetus birth weight. Each live fetus was recorded at each gestation day from each group.

## QUANTIFICATION AND STATISTICAL ANALYSIS

We used paired two-tailed t tests (difference between two groups) or unpaired two-tailed t tests to determine statistical significance ( $p < 0.05$  was considered significantly different). The specific statistical parameters were represented in the Figure Legend of each Figure. All of the data were presented as Mean  $\pm$  SEM, \* $p < 0.05$ , \*\* $p < 0.01$ , \*\*\* $p < 0.005$ , \*\*\*\* $p < 0.0001$ .

## DATA AND SOFTWARE AVAILABILITY

The data that support the findings of this report are available from the corresponding authors upon reasonable request.

For analysis of differences in genes expressions in CD49a<sup>+</sup>NK and CD49a<sup>-</sup>NK cells, CD49a<sup>+</sup>NK cells (Gated CD56<sup>+</sup>CD3<sup>-</sup>CD45<sup>+</sup>CD49a<sup>+</sup>CD49b<sup>-</sup>) were sorted from the healthy deciduas from the first trimester; CD49a<sup>-</sup>NK cells (Gated CD56<sup>+</sup>CD3<sup>-</sup>CD45<sup>+</sup>CD49a<sup>-</sup>CD49b<sup>+</sup>) were sorted from the peripheral blood of healthy donors. The sorting was done by FACS Aria (BD Bioscience). Microarray analysis using the Affymetrix Human Gene Expression Array (GSE24268) compared sorted CD49<sup>+</sup>NK and CD49<sup>-</sup>NK cells. The log ratio of the green to red intensities for each signal was used for statistical analyses. Microarray data have been deposited at the National Center for Biotechnology Information GEO repository through accession number GSE97217.